Comparative Cr and Mn speciation across a shore-to-reef gradient in lagoon sediments downstream of Cr-rich Ferralsols upon ultramafic rocks in New Caledonia

Pauline Merrot, Farid Juillot, Pierre Le Pape, Pierre Lefebvre, Jessica Brest, Isabelle Kieffer, Nicolas Menguy, Eric Viollier, Jean-Michel Fernandez, Benjamin Moreton, et al.

Journal of Geochemical Exploration 229 (2021) 106845

https://doi.org/10.1016/j.gexplo.2021.106845

Received 18 September 2019; Received in revised form 11 May 2021; Accepted 13 June 2021

Available online 16 June 20210375-6742/

Comparative Cr and Mn speciation across a shore-to-reef gradient in lagoon sediments downstream of Cr-rich Ferralsols upon ultramafic rocks inNew Caledonia

Pauline Merrot [a], Farid Juillot [a, b, *], Pierre Le Pape [a], Pierre Lefebvre [a], Jessica Brest [a], Isabelle Kieffer [c, d], Nicolas Menguy [a], Eric Viollier [e], Jean-Michel Fernandez [f], Benjamin Moreton [f], Olivier Radakovitch [g], Guillaume Morin [a]

[a] *Institut de Min´eralogie, de Physique des Mat´eriaux et de Cosmochimie (IMPMC), Sorbonne Universit´e, UMR 7590 CNRS, MNHN, IRD, 75252 Paris Cedex 5, France* [b] *Institut de Recherche pour le D´eveloppement (IRD), ERL 206 IMPMC, 98848 Noum´ea, New Caledonia*[c] *Observatoire des Sciences de l'Univers de Grenoble (OSUG), Universit´e Grenoble-Alpes, UMR 832 CNRS, F-38041 Grenoble Cedex 9, France*[d] *BM30B/CRG-FAME, ESRF, Polygone scientifique, 38000 Grenoble, France*

[e] *Institut de Physique du Globe de Paris (IPGP), Universit´e de Paris, UMR CNRS 7154, 75005 Paris, France*[f] *Analytical Environmental Laboratory (AEL), 98800 Noum´ea, New Caledonia*[g] *Aix-Marseille Universit´e, CNRS, IRD, INRAE, Coll. France, Centre Europ´een de Recherche et d'Enseignement des G´eosciences de l'Environnement (CEREGE), 13080 Aix- en-Provence, France*

Keywords:

Lagoon Sediments Chromium Manganese Speciation

ABSTRACT

Ferralsols upon ultramafic rocks are among the most Cr-enriched soils at the Earth surface. Weathering and erosion of these soils represents a major source of Cr for coastal sediments downstream of ultramafic settings. Although Cr mainly occurs as Cr(III)-bearing chromite and Fe-(hydr)oxides in Ferralsols upon ultramafic rocks, several evidences of oxidized Cr(VI) in relation with Mn-oxides have been reported. Regarding the high solubility and toxicity of this latter Cr species, a thorough characterization of Cr and Mn crystal-chemistry in tropical sedimentary settings downstream of Ferralsols upon ultramafic rocks is needed to evaluate the potential threat towards the biodiversity of these coastal environments. In this study, we determined Cr and Mn speciation across a shore-to-reef gradient in lagoon sediments downstream of one of the largest lateritized ultramafic regolith in New Caledonia that contains up to 5 wt% Cr_2O_3. Chromium K-edge XANES data emphasized the absence of Cr (VI) and indicated a major hosting of Cr by chromite and clay minerals close to the shore, whereas Cr-bearing goethite dominated Cr speciation close to the reef. Manganese K-edge XANES data indicated a major hosting of Mn by clay minerals close to the shore, whereas Mn-carbonates dominated Mn speciation close to the reef. The lack of Mn-oxides detection was considered to explain the absence of Cr(VI) in the studied sediments. This result thus suggests that, despite their shallow character that can favor occasional re-oxidation of the top-layer sedi- ments upon re-suspension events, lagoon sedimentary settings downstream of Cr-rich Ferralsols upon ultramafic rocks appear rather favorable to Cr sequestration as the less mobile and less toxic Cr(III) form. However, the reverse trends observed from the shore to the reef between the chromite and goethite contributions to Cr speciation, as well as the decrease of the Cr/Ti ratio, suggest that a fraction of Cr could have been released towards the water column upon partial weathering of chromite to goethite during sediments transport across the shore-to-reef gradient. This latter point emphasizes the potential hazard that could still represent Cr for the exceptional biodiversity of tropical lagoon ecosystems downstream of Cr-rich Ferralsols, despite the absence of detectable Cr(VI). It thus calls for further studies aimed at better evaluating the stability of Cr(III)-bearing mineral phases upon early diagenesis in these shallow sedimentary settings.

1. Introduction

Although many anthropogenic activities contribute to chromium (Cr) sources in the environment, this trace metal naturally occurs at trace levels in the Earth crust (100 $mg \cdot kg^{-1}$ on average; Nriagu, 1988; Wedepohl, 1995). The highest Cr concentrations (*i.e.* 2500–3000 $mg \cdot kg^{-1}$) are found in ultramafic rocks (Nriagu, 1988; Wedepohl, 1995) and weathering of these rocks under tropical climate can yield Ferralsols with Cr concentration up to several wt% Cr_2O_3, which is far above the highest Cr concentration reported for other soils (*i.e.* around 4000 $mg \cdot kg^{-1}$; Burt et al., 2003; Oze et al., 2004). Regarding the known toxicity of this trace metal, such large amounts of Cr in Ferralsols upon ultramafic rocks can represent a potential threat towards the biodiver- sity of related ecosystems. However, Cr toxicity and mobility depend on its redox state (Jacobs and Testa, 2005; Rai et al., 1989). Since Cr(III) compounds such as chromium trioxide Cr_2O_3 and chromite $FeCr_2O_4$ are weakly soluble (Motzer, 2005; Jacobs and Testa, 2005), the reduced form of Cr is considered less toxic and weakly mobile (Guertin, 2005; Jacobs and Testa, 2005). On the opposite, Cr(VI) (*i.e.* the oxidized form of Cr) is essentially found as the highly soluble chromate oxyanion $CrO^{2}{}_{4}^{-}$ (Zhitkovich, 2011; Jacobs and Testa, 2005; Motzer, 2005), which is toxic and carcinogenic (*i.e.* maximum concentration limit in drinking water fixed at 50 μg/L by the World Health Organization, 2011). In addition, several reactions have already demonstrated their capacity to modify the redox state of Cr in natural systems. The soluble and toxic Cr (VI) can be reduced to insoluble Cr(III) upon sorption to Fe(II,III)-(hydr) oxides such as magnetite (He and Traina, 2005; Kendelewicz et al., 2000; Peterson et al., 1997; Fendorf and Li, 1996) and green rust (Wil- liams and Scherer, 2001; Loyaux-Lawniczak et al., 2000), but also Fe(II)- sulfides (Doyle et al., 2004; Kim et al., 2002a; Patterson et al., 1997), Fe (II)-bearing clay minerals (Taylor et al., 2000; Bishop et al., 2014, 2019; Joe-Wong et al., 2017; Qafoku et al., 2017) and organic matter (Szulc- zewski et al., 2001). On the opposite, direct oxidation of Cr(III) to Cr(VI) by dissolved O_2 in natural systems is possible but limited because of its very low kinetics (Eary and Rai, 1987). However, Cr(III) can be readily oxidized to Cr(VI) upon reaction with Mn(IV)-oxides surfaces (Landrot et al., 2010, 2012; Oze et al., 2007; Apte et al., 2006; Feng et al., 2007; Motzer, 2005; Kim et al., 2002b; Ko˘zuh et al., 2000; Nico and Zasoski, 2000; Banerjee and Nesbitt, 1999; Fendorf et al., 1992; Fendorf, 1995; Manceau and Charlet, 1992; Eary and Rai, 1987) owing to the high redox potential and strong sorption capacity of these mineral phases (McKenzie, 1989). As a consequence, a thorough characterization of the molecular level speciation of both Cr and Mn is required for evaluating the potential threat towards biodiversity, when both trace metals occur simultaneously in Cr-rich natural systems.

Such a context of Cr and Mn co-occurrence is notably found in New Caledonia, where Ferralsols that have developed upon ultramafic rocks exhibit high concentrations of these two trace metals (up to 6 wt% Cr_2O_3 and 4.5 wt% MnO; Becquer et al., 2006; Fandeur et al., 2009a; Dublet et al., 2012). In previous studies, mineralogical analyses of these Fer- ralsols revealed the occurrence of Mn(IV-III)-oxides (Fandeur et al., 2009a; Dublet et al., 2012; Quantin et al., 2002) and spectroscopic an- alyses of the redox state of Cr indicated the occurrence of Cr(VI) sorbed to goethite in specific levels enriched in these Mn(IV-III)-oxides (Fan- deur et al., 2009a). Besides, Cr was found to mostly occur as chromite $(Fe,Mg)(Cr,Al)_2O_4$ that showed evidences of deep weathering (Fandeur et al., 2009b). In the geomorphological context of New Caledonia, erosion of these Ferralsols during tens to hundreds of thousand years thus have brought large amounts of Cr(III)-bearing phases, together with Mn(IV-III)-oxides, towards downstream sediments of the New Caledonia lagoon that is partially registered as a World Heritage (UNESCO, 2008). In this coastal sedimentary setting, the anaerobic conditions that develop upon early diagenesis are expected to stabilize Cr(III)-bearing phases and to promote the biologically driven dissolution of Mn(IV- III)-oxides (Shaw et al., 1990; Burdige, 1993; Canfield et al., 1993; Davison, 1993; Thamdrup et al., 1994; Wang and Van Cappellen, 1996;

Slomp et al., 1997). The shallow lagoon sedimentary setting of New Caledonia should thus be favorable to Cr sequestration as the less toxic and mobile Cr(III), which should not represent a potential hazard. However, the significant amounts of dissolved organic ligands that can be released upon early diagenesis and/or inherited from the upstream mangrove sediments could also promote the formation of Cr(III)-organic complexes that could trigger Cr(III) oxidation to Cr(VI) by enhanced mobilization towards the water column (James and Bartlett, 1983; Richard and Bourg, 1991; Fendorf, 1995; Puzon et al., 2005, 2008; Gustafsson et al., 2014; Fan et al., 2019). In addition, a fraction of dis- solved Mn(II) produced after the reductive dissolution of Mn(IV-III)- oxides could be biologically recycled as Mn(IV-III)-oxides upon tran- sient re-oxidation of the upper sediments layers (Tebo et al., 2004, 2005; Bargar et al., 2005; Webb et al., 2005). The biogeochemical cycling of Cr and Mn upon early diagenesis in the specific context of the shallow lagoon environment downward of Cr-rich Ferralsols in New Caledonia thus deserves to be investigated in order to better evaluate the potential threat towards the biodiversity of this exceptional coastal environment.

The objective of the present study was to address this issue by investigating the potential evolution of the Cr and Mn host minerals, as well as of the redox state of Cr, upon early diagenesis in the lagoon sediments downstream of Cr-rich Ferralsols in New Caledonia. For that purpose, we have sampled three sediments cores across a shore-to-reef gradient in a lagoon bay located downstream of one of the largest lat- eritized ultramafic regolith from New Caledonia (Koniambo, Northern Province) and we have combined X-ray Absorption Spectroscopy (XAS), X-Ray Diffraction (XRD) and Transmission Electron Microscopy (TEM) to identify and quantify the Cr and Mn species as a function of both the distance from the shore and the depth along each core.

2. Materials and methods

2.1. Sampling site and sampling procedure

New Caledonia is located in the South-West Pacific Ocean and the main island (Grande Terre-20° S-23° S) extends over ~500 km long and ~50 km wide (Fig. 1) under tropical climate. The studied lagoon is located on the North-West of New Caledonia (Voh-Kone-Pouembout VKP area, Norther Province; Fig. 1). Sediments were collected down- stream of the Koniambo regolith, one of the major lateritic regoliths on the West coast of New Caledonia where open-cast mining has been operating sporadically for the last 150 years, with an industrialization in the early 2010's. Erosion of lateritic materials (including Ferralsols developed on ultramafic rocks at the top of the Koniambo regolith) are thus considered as a source for the studied lagoon sediments. In addi- tion, as shown in a previous study by Merrot et al. (2019), other geological/pedological settings like Cambisols, Vertisols and Acrisols developed on volcano-sedimentary rocks have also to be considered as natural sources of detrital inputs towards the studied lagoon sediments (Fig. 1). The sampling campaign was realized in July 2016 during the dry season in the Vavouto Bay, which is located downstream of the deeply weathered ultramafic Koniambo regolith (20° 59′ S; 164° 49′ E). Three sediments cores of about 20 cm long were collected, one close to the shore, one half way between the shore and the reef and one close to the coral reef (Fig. 1). Considering an average sedimentation rate of ~0.30 mm/year estimated on the basis of ^{210}Pb measurements per- formed on sediments cores collected at other locations in the studied VKP lagoon (Merrot et al., 2019), the maximum age of the studied sediments cores is estimated to ~60 years. To prevent oxidation of the sediments, each core was preserved with its top water at room tem- perature. As reported in Merrot et al. (2019), O_2 micro-profiling ex- periments indicated anoxic conditions below 5 mm depth. For each core, sediment samples were collected every cm under nitrogen flow, no longer than 3 h after cores collection. Each sediment sample was immediately stored under anoxic conditions at 4 °C in glass vials sealed with a butyl rubber stoppers. The vials were re-opened at the laboratory

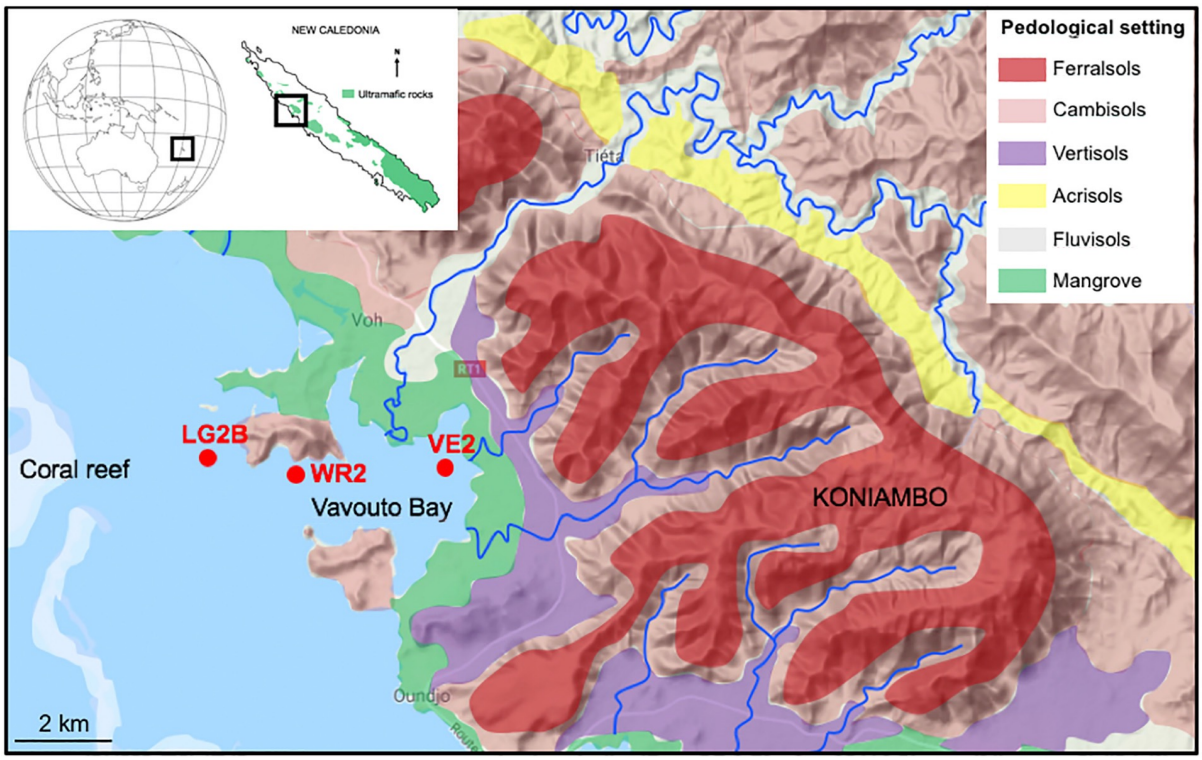

Fig. 1. Map of the studied area showing the sediment core sampling locations (VE2, WR2 and LG2B cores) in the Vavouto Bay displayed on a topographic map of the studied area (source: google.com) with schematic pedological setting after Fritsch (2012) superimposed.

in a glove box under N_2 atmosphere ($[O_2] \leq 1$ ppm) for vacuum-drying. Each sediment sample was then ground with a mechanical grinder at a 30 Hz frequency during 20 min and stored under anoxic conditions in sealed vials in the glove box until chemical and spectroscopic analyses (Merrot et al., 2019).

2.2. Chemical, mineralogical and granulometric analyses

Bulk concentration of major (Ca, Mg, Na, K, Ti, Fe, Al and Si) and trace (Co, Cr, Mn, Ni, Cu, P and Zn) elements were determined by ICP- OES (VARIAN® 730ES ICP optical emission spectrometer) and ICP-MS (PERKIN ELMER® NexION 350× ICP mass spectrometer) after alka- line fusion, by the Laboratoire des Moyens Analytiques (LAMA-IMAGO, IRD, Noumea, New-Caledonia). This laboratory is ISO 9001 certified and member of the Global Soil Laboratory Network that was established in 2017 by the Food and Agriculture Organization (FAO) to respond to the need for harmonizing worldwide soil analytical data (http://www.fao. org/global-soil-partnership/glosolan/en/). Chemical analyses per- formed on the WEPAL 986 Sandy Soil Certified Reference Material are reported in Table S1. The mineralogical composition of the studied lagoon sediments was characterized at the Institut de Physique des Materiaux et de Cosmochimie (IMPMC, Paris, France) by X-ray powder diffraction (XRD) with a PANALYTICAL® X'Pert Pro diffractometer equipped with an X'celerator detector and using Co Kα radiation in order to minimize X-ray absorption by Fe. Clay minerals were characterized by TEM-EDXS analyses at IMPMC by using a JEOL 2110F TEM equipped with a JEOL EDXS Si(Li) detector at 200 kV. The results of these mineralogical analyses were detailed in (Merrot et al., 2019). Granulo- metric analyses were performed along the three studied cores at the Centre Europeen de recherche et d'Enseignement des Geosciences de l'Environnement (CEREGE, Aix-en-Provence, France) using a Beckman Coulter LS 13320 laser particle size analyzer. Before each analysis, the sediments were stirred during 15 min in a sodium

hexametaphosphate solution for de-flocculation.

2.3. Statistical analyses

A Principal Component Analysis (PCA) was performed on the chemical composition of the studied sediments (*i.e.* Ca, K, Mg, Na, Si, Al, Fe, Ti, Cr, Mn, Co and Ni concentrations) in order to evidence possible associations among the concentrations of major and trace elements and simplifying the dataset by reducing the number of variables into major components. This analysis was performed with the R software (R Core Team, 2020), using the "FactoMineR" package, available at the following link: http://CRAN.R-project.org/package=FactoMineR.

2.4. X-ray absorption spectroscopy (XAS) data collection

Cr and Mn K-edges X-ray Absorption Near-edge Structure (XANES) data were collected on a set of 6 sediment samples selected at two depths in each of the three cores (1–2 cm and 16.5–17.5 cm depths for core VE2, 1–2 cm and 19.5–20.5 cm depths for core WR2 and 1–2 cm and 17.5–18.5 cm depths for core LG2B). For each sample, XANES spectra at both the Cr K-edge (5950 to 6150 eV) and Mn K-edge (6500 to 6650 eV) were collected consecutively without changing the sample. XANES spectra were collected at liquid He temperature (10– 20 K) and in fluorescence mode using a Canberra® high-throughput Ge-30-elements on the bending magnet FAME beamline at the European Synchrotron Radiation Facility (ESRF, Grenoble, France). The energy of the incoming beam was selected with a Si(220) double-crystal monochromator and calibrated by setting the first inflection point of the Mn K-edge of a metallic Mn foil to 6539 eV. For these measurements, finely ground and homogenized pure samples were prepared as pressed pellets and mounted on the sample holder in a glove box under N_2 atmosphere before being carried to the synchrotron facilities in anoxic containers. Once at the synchrotron, all the sample holders were stored in a glove bag under N_2 atmosphere before being mounted on the cryostat sample rod at the beamline and immediately introduced into the cryostat. For each sample, between 2 and 10 scans were necessary to obtain an acceptable signal-to-noise ratio.

2.5. X-ray Absorption Spectroscopy (XAS) data analysis

XANES data were averaged, calibrated and normalized with the ATHENA code (Ravel and Newville, 2005). Normalized data were then analyzed by principal component analysis (PCA) using the SIXPACK code (Webb, 2005). The minimum number of principal components necessary to fit each set of sediment samples spectra was chosen on the basis of the minimum value of the factor indicator function (Malinowski, 1978, 1987, 1991; Webb, 2005) and of the quality of the reconstruction with up to the three first principal components. Target Transformation (TT) was then used to select the model compounds spectra that were further used in the linear combination least-square fitting (LC-LSF) of the sediment spectra. LC-LSF analysis was realized with the ATHENA software (Ravel and Newville, 2005) using model compounds spectra retrieved by PCA-TT analysis as fitting components. LC-LS fits were performed on the normalized XANES spectra over the 5985–6065 eV range for Cr K-edge XANES spectra and the 6530–6600 eV range for Mn K-edge XANES spectra. The quality of the LC-LS fit was estimated using a *R*-factor of the following form: $Rf = \Sigma[k^3\chi(k)_{exp} - k^3\chi(k)_{calc}]^2 / \Sigma[k^3\chi(k)_{exp}]^2$.

In addition to quantitative analysis of Cr speciation, the pre-edge region of Cr K-edge XANES spectra was also used to determine the redox state of Cr, since tetrahedral Cr(VI) is characterized by a strong absorption peak at 5993 eV in the pre-edge region (Huggins et al., 1999), whereas octahedral Cr(III) yields only two weak peaks at 5990 and 5993 eV (Gaudry et al., 2007; Juhin et al., 2008). For that purpose, the pre- edge region (5985–6000 eV) of the Cr K-edge XANES spectra was extracted by fitting the background of the main edge to an arctangent function (Huggins et al., 1999). The resulting data were

then compared either to those from $Cr^{VI}O_2/Cr^{III}_2O_3$ synthetic mixtures with 0 or 5% Cr (VI) (see Fandeur et al., 2009a for further details on the preparation procedure of these synthetic samples) or from the model compounds used for the LC-LS fits of experimental Cr K-edge XANES data.

2.6. Model compounds for XAS analyses

Our database of Cr K-edge reference spectra included experimental data from natural compounds such as chromite [$FeCr_2O_4$], Cr-bearing serpentine [$(Mg,Fe,Cr)_3Si_2O_5(OH)_4$] and volkonskoite [$Ca_{0.3}(Cr,Mg,Fe,Mn)_2(Si,Al)_4O_{10}(OH)_2{\cdot}4H_2O$] and synthetic compounds such as Cr- bearing goethite [α-(Fe,Cr)O(OH)] and hematite [$(Fe,Cr)_2O_3$] (Fan- deur et al., 2009b). In addition to these already available XANES spectra, the Cr K-edge spectra of a synthetic Cr-bearing pyrite ($(Fe,Cr)S_2$ (1wt% Cr_2O_3) and synthetic Cr-citrate were also collected on the SAMBA beamline at the Source Optimis´ee de Lumi`ere d'Energie Interm´ediaire du LURE synchrotron (SOLEIL, Saint-Aubin, France) using the same experimental setup than the sediments samples.

Our database of Mn K-edge reference spectra included experimental data from synthetic compounds such as Mn-bearing goethite [α-(Fe,Mn) O(OH)], Mn-bearing clay minerals (serpentine [$(Mg,Mn)_3Si_2O_5(OH)_4$] and kerolite [$(Mg,Mn)_3Si_4O_{10}(OH)_2{\cdot}nH_2O$]), manganite [MnOOH], but also natural compounds such as Mn-oxides (Na-brinessite [Na_xM- $n_2O_4.1.5H_20$] and asbolane [$(Ni,Co)_{2-x}(MnO_2)_{2-y}(OH)_{2-2y+2x}.nH_20$]), Mn-bearing clay minerals (serpentine [$(Mg,Fe,Ni,Mn)_3Si_2O_5(OH)_4$] and volkonskoite [$Ca_{0.3}(Cr,Mg,Fe,Mn)_2(Si,Al)_4O_{10}(OH)_2{\cdot}4H_2O$]) and Mn- bearing forsterite [Mg_2SiO_4] (Dublet et al., 2017). In addition to these already available XANES spectra, the Mn K-edge spectrum of a crystal- line Mn-bearing calcite [$(Ca,Mn)CO_3$] (3150 ppm Mn) from a fracture infillings in the Toarcian deposit of Tournemire (Cantal, France) was also collected on a finely ground sample in transmission detection mode at 80 K on the XAFS beamline at Elettra Synchrotron (Trieste, Italy).

3. Results

3.1. Mineralogical and granulometric characteristics of the studied sediments

The mineralogical composition of the studied sediments has been extensively assessed in a previous study focused on sulfur, iron and nickel speciation in the same sediments (Merrot et al., 2019). Briefly, XRD data indicate that the sediments close to the shore (VE2) consist of quartz, albite, various phyllosilicates (*i.e.* smectite, illite/muscovite, chrysotile, greenalite/berthierine) and minor amounts of pyrite. In contrast, the sediments close to the coral reef (LG2B) consist of aragonite [$CaCO_3$], magnesian calcite [$(Mg,Ca)CO_3$] and calcite [$CaCO_3$], together with minor amounts of the silicate minerals observed in the sediments close to the shore. Finally, the sediments sampled at the intermediate location (WR2) exhibit a mixed mineralogical composition (Fig. S1; Merrot et al., 2019). The first important mineralogical feature of the studied sediments is thus the minor contribution of Fe- and/or Mn- oxides, despite their location downstream of the Koniambo lateritic regolith (Fig. 1). The second important mineralogical feature of these sediments is their small pyrite contents. On that perspective, a previous study that used XAS data at the *S* K-edge revealed a decreasing contri- bution of sulfides to S speciation across the shore-to-reef gradient with about 90% of total S as sulfides in the sediments close to the shore and about 40% of total S as sulfides in the sediments close to the reef (Merrot et al., 2019). The third important mineralogical feature of the studied sediments is an increase of the carbonate minerals contribution, together with a decrease of the silicate minerals one, across the shore-to- reef gradient. Finally, the last important feature is that the mineralogical composition of the studied sediments does not change significantly with depth (Merrot et al., 2019).

Regarding the low variability of the sand, silt and clay fractions along each core (*i.e.* low standard deviation; Table S2), the granulometric characteristics of the studied sediments can be described by considering their mean values at each location. Following this procedure, the major granulometric feature of the studied sediments is their silty composition (*i.e.* mean silt fraction ranging from 62 to 83%; Table S2). Beyond this major feature, some differences from one core to the other can be emphasized, depending on the granulometric fraction considered. The silty fraction is larger in the sediments at the intermediate position (*i.e.* 83% for WR2, compared to 62% for VE2 and 67% for LG2B; Table S2). The sandy fraction is larger in the sediments close to the shore (*i.e.* 36% for VE2, compared to 13 wt% for WR2 and 22% for LG2B; Table S2). Finally, the clayey fraction is larger in the sediments close to the reef (*i.e.* 10% for LG2B, compared to 3% for VE2 and 4% for WR2; Table S2). Considering these differences from one core to the other, the global granulometric trend that can be considered for the studied sediments is an increase of the clayey fraction, and a concomitant decrease of the sandy fraction, from the shore to the reef.

3.2. Cr and Mn concentrations in the studied sediments

At the exception of Mn in the sediments close to the shore (VE2), Cr and Mn concentrations do not show any significant variation with depth (Fig. 2; Table S3). This result is in agreement with the low variation of the mineralogical composition along the three studied sediment cores revealed by XRD data (Merrot et al., 2019). Mean concentrations can thus be used to describe the chemical trends of Cr and Mn across the shore-to-reef gradient. On that perspective, both Cr and Mn show similar decreasing concentrations across the shore-to-reef gradient (Fig. 2; Table S3). However, two major differences in the chemical trends of both trace metals can be emphasized.

First, Cr concentrations in the sediments close to the shore (VE2) are significantly higher (*i.e.* mean value at 1512 ± 260 $mg{\cdot}kg^{-1}$; Fig. 2; Table S3) than Mn concentrations (*i.e.* mean value at 445 ± 110 $mg{\cdot}kg^{-1}$; Fig. 2; Table S3). Chromium concentrations are within the range of those reported for other lagoon sediments downstream of lateritic regoliths in New Caledonia (*i.e.* from 450 to 3200 $mg{\cdot}kg^{-1}$; Ambatsian et al., 1997; Dalto et al., 2006), but significantly higher than those reported for lagoon sediments downstream of non-lateritic geological settings in New Caledonia (*i.e.* from 50 to 800 $mg{\cdot}kg^{-1}$; Ambatsian et al., 1997; Dalto et al., 2006). On the opposite, Mn con- centrations in the sediments close to the shore are in the range of those reported for other lagoon sediments downstream of non-lateritic geological settings in New Caledonia (*i.e.* from 100 to 400 $mg{\cdot}kg^{-1}$; Ambatsian et al., 1997; Dalto et al., 2006), but significantly lower than those reported for other lagoon sediments downstream of lateritic reg- oliths in New Caledonia (*i.e.* from 300 to 1900 $mg{\cdot}kg^{-1}$; Ambatsian et al., 1997; Dalto et al., 2006). This difference can be explained by the significantly higher Cr concentrations in the Ferralsols at the top of the Koniambo regolith compared to Mn concentrations (*i.e.* 2.1–4.0 wt% Cr_2O_3 compared to 0.2–1.1 wt% MnO; Fandeur et al., 2009a,b; Dublet et al., 2012, 2015; Ulric et al., 2019). Although volcano-sedimentary formations also contribute to the geological setting around the Koniambo regolith, the related soils (*i.e.* Cambisols and Vertisols; Fig. 1; Fritsch, 2012) do not show significant differences between Cr and Mn concentrations(*i.e.*340–1500$mg{\cdot}kg^{-1}$forCrand820–1000$mg{\cdot}kg^{-1}$for Mn; Vincent et al., 2018). The contribution of these soils to trace metals inputs towards the sediments in the Vavouto Bay can thus not explain the higher Cr concentrations in the sediments close to the shore, which are thus mainly attributed to the continental inputs related to the Fer- ralsols at the top of the Koniambo regolith.

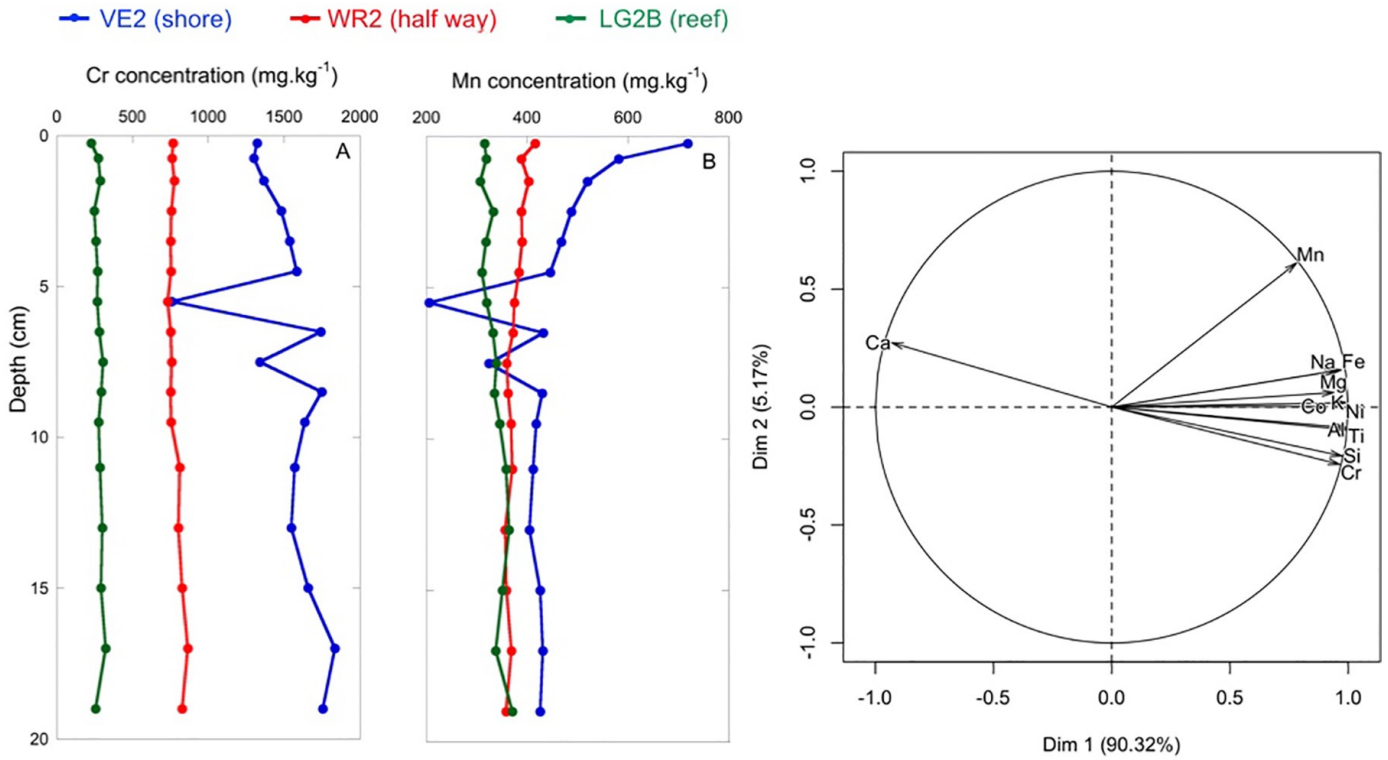

Fig. 2. (Left) Vertical evolution of Cr and Mn concentrations along the sediment cores collected close to the shore (VE2; blue), half way between the shore and the reef (WR2; red) and close to the reef (LG2B; green) in the Vavouto Bay. (Right) Results of the PCA performed on the chemical composition of the studied sediments showing the loading of the variables (*i.e.* Ca, K, Mg, Na, Si, Fe, Mn, Al, Cr, Ni, Co and Ti concentrations) on the PCA factors 1 and 2 (representing more than 95% of the variance of the dataset). (For interpretation of the references to colour in this figure legend, the reader is referred to the web version of this article.)

Second, the decrease of the concentrations across the shore-to-reef gradient in the studied sediments is less marked for Mn than for Cr. This difference suggests that continental inputs might be less important for Mn than for Cr and that an additional marine source could contribute for Mn. This hypothesis is supported by the results of a Principal Com- ponents Analysis (PCA) performed on Ca, K, Mg, Na, Si, Al, Fe, Ti, Cr, Mn, Co and Ni concentrations, which indicated a clustering of K, Mg, Na, Si, Al, Fe, Ti, Cr, Co and Ni loadings on the two first factors (*i.e.* 95.49% of the cumulative variance explained, with 90.32% for factor 1 and 5.17% for factor 2), whereas Ca loaded oppositely and Mn loaded intermediately (Fig. 2). The opposite correlation between K, Mg, Na, Si,

Al, Fe, Ti, Cr, Co and Ni on the one hand, and Ca on the other hand, was confirmed by Pearson correlation analysis (Table S4). This analysis also confirmed the intermediate opposite correlation between Mn and Ca (Table S4). Regarding the known occurrence of these major and trace elements in the continental crust, the clustering of K, Mg, Na, Si, Al, Fe, Ti, Cr, Co and Ni loadings is considered to represent the continental inputs in the Vavouto Bay. On the opposite, regarding the known major contribution of carbonate minerals to shallow marine sediments, the loading of Ca is considered to represent the marine inputs in the Vavouto Bay. Following this classification, the intermediate loading of Mn be- tween these two end-members strongly suggests a mixed continental and marine contribution to the inputs of this trace metal towards the studied sediments.

The abovementioned differences in the chemical trends of Cr and Mn across the shore-to-reef gradient suggest contrasted sources apportion- ment for these two trace metals in the Vavouto Bay, with a major con- tinental contribution for Cr and a mixed continental and marine contribution for Mn.

3.3. XAS-derived Cr speciation

A PCA analysis was performed on the Cr K-edge XANES spectra of the 6 studied sediment samples. The minimum value of the indicator func- tion during this PCA analysis suggested that 3 components were necessary to reconstruct the whole set of the Cr K-edge XANES sediment data (Fig. S2). Then, a TT analysis performed on our range of model compounds indicated Cr-bearing clay minerals (*i.e.* volkonskoite and Cr- bearing serpentine, halloysite and kaolinite), as well as chromite and Cr- bearing goethite and ferrihydrite, as the most relevant model com- pounds for the LC-LSF analysis of experimental Cr K-edge data (Fig. 3; Table S5). Among these candidate model compounds, chromite yielded the lowest chi-square value (Fig. 3; Table S5). Since this mineral species was also identified by Fandeur et al. (2009b) as a major Cr species in the Koniambo lateritic regolith, it was considered as a fully relevant LC-LSF component to analyze our experimental Cr K-edge XANES data of sediment samples. On the opposite, volkonskoite (*i.e.* a Cr-rich smectite) and Cr-bearing serpentine yielded the lowest chi^2 values among the

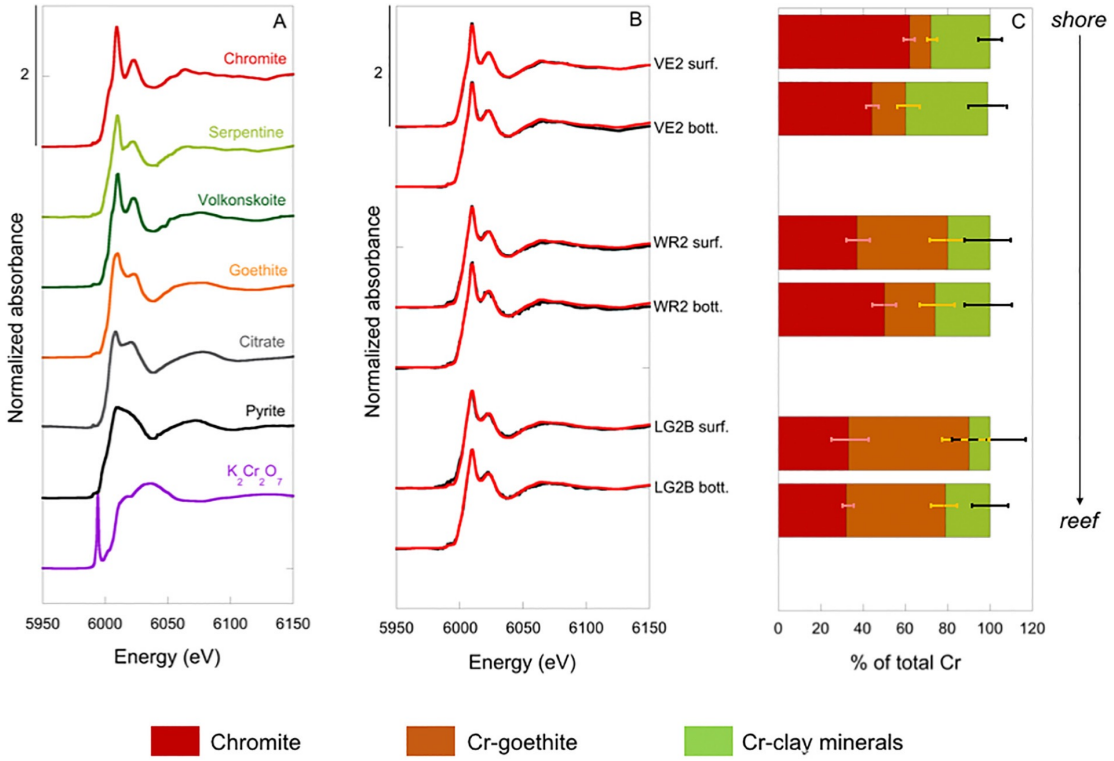

Fig. 3. Cr K-edge XANES spectra of (A) the model compounds used for the LC-LSF analysis and (B) the lagoon sediment samples (experimental data in black and LC- LS fits in red). The quantitative results of the LC-LS fits on Cr speciation are shown in (c). Surface samples correspond to 1–2 cm depth for the three cores. Bottom samples correspond to 16.5–17.5 cm depth for core VE2, 19.5–20.5 cm depth for core WR2 and 17.5–18.5 cm depth for core LG2B. (For interpretation of the references to colour in this figure legend, the reader is referred to the web version of this article.)

candidate Cr-bearing clay minerals model compounds submitted to TT analysis (Fig. 3; Table S5). However, in a preliminary study (Merrot et al., 2019), TEM-EDXS analyses revealed the occurrence of Cr in 1/1 clay minerals identified as chrysotile and greenalite/berthierine, but also in 2/1 clay minerals identified as Fe-rich smectite. Since comple- mentary TEM-EDXS analyses performed during the present study confirmed these preliminary observations (Fig. S3), Cr-bearing serpen- tine was considered as a relevant proxy for Cr in trioctahedral 1/1 clay mineral in the studied sediments, whereas volkonskoite was considered as a relevant proxy for Cr in dioctahedral 2/1 smectite. Finally, since preliminary SEM-EDXS and TEM-EDXS analyses also reported the presence of trace amounts of Cr in goethite (Merrot et al.,

2019) and complementary TEM-EDXS analyses confirmed these findings, the Cr- bearing goethite model compound retrieved by the TT analysis (Table S5) was also considered as a component for LC-LSF analysis of the Cr K-edge XANES spectra of the studied sediments.

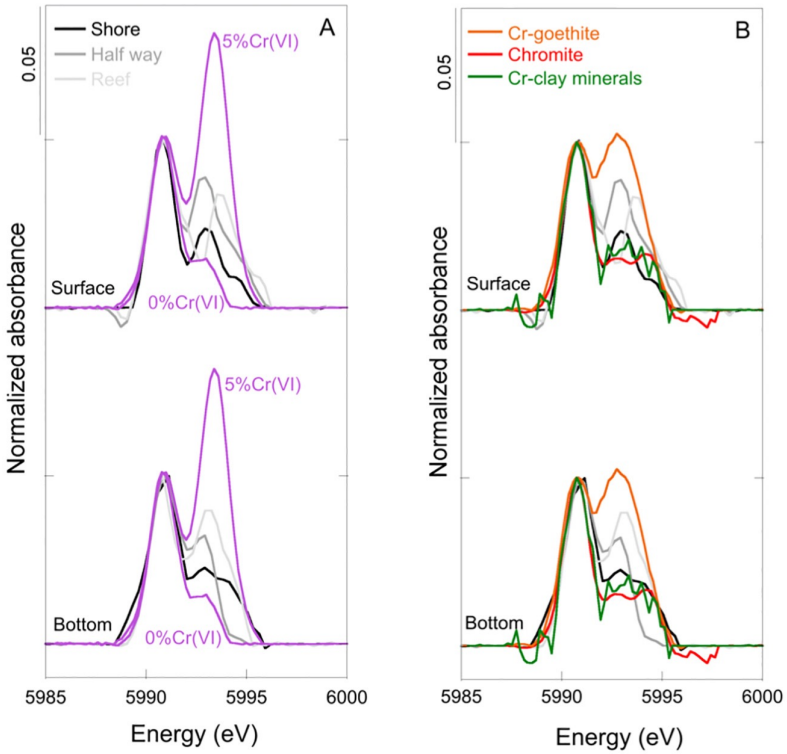

Fig. 4. Comparison of the pre-edge peaks of the normalized Cr K-edge XANES spectra from the studied sediments with those from (A) synthetic $Cr^{VI}O_2/Cr^{III}_2O_3$ mixtures containing 0% and 5% Cr(VI) and (B) the model compounds used in the PCA procedure. Further details on the interpretation of the pre- edge peaks of the normalized Cr K-edge XANES spectra of the model compounds can be found in Fandeur et al. (2009a). Surface samples correspond to 1–2 cm depth for the three cores. Bottom samples correspond to 16.5–17.5 cm depth for core VE2, 19.5–20.5 cm depth for core WR2 and 17.5–18.5 cm depth for core LG2B.

The best LC-LS fits of the normalized Cr K-edge XANES spectra of the studied sediments were obtained using chromite, Cr-bearing goethite and Cr-bearing serpentine as fitting components (Fig. 3; Table S6). Note that within our uncertainty range, volkonskoite could have been used instead of Cr-bearing serpentine for the VE2 samples and the WR2 sur- face sample, resulting in a similar fit quality. However, this model compound did not match the Cr K-edge XANES spectra of the WR2 bottom sample and the LG2B samples. The Cr-bearing serpentine model compound was thus chosen as the most representative clay mineral model compound to fit the Cr K-edge XANES spectra of the studied sediments. Following this procedure, the LC-LSF fits of the normalized Cr K-edge XANES spectra indicated some significant variations in the contribution of chromite, goethite and Cr-bearing clay minerals to Cr speciation across the shore-to-reef gradient (Fig. 3; Table S6). The contributions of chromite and Cr-bearing clay minerals to Cr speciation were found to dramatically decrease from the shore to the reef (*i.e.* respectively from 62 to 33% of Cr speciation and from ~34 to 15% of Cr speciation; Fig. 3; Table S6), whereas that of goethite strongly increased (*i.e.* from 9 to 58% of Cr speciation; Fig. 3; Table S6). Chromite thus dominates Cr speciation in the sediments close to the shore (VE2), whereas Cr-bearing goethite dominates in the sediments close to the coral reef (LG2B; Fig. 3; Table S6). Hence, the increase of the Cr-bearing goethite contribution at the expense of the chromite and Cr-bearing clay minerals contributions appears as the

major trend in the evolution of Cr speciation across the shore-to-reef gradient. Although they could be considered as significant according to the fit uncertainties, the slight changes in the contributions of the various Cr-bearing species to Cr speciation observed along each sediment core were not considered as an actual trend given the limited number of samples analyzed for Cr speciation.

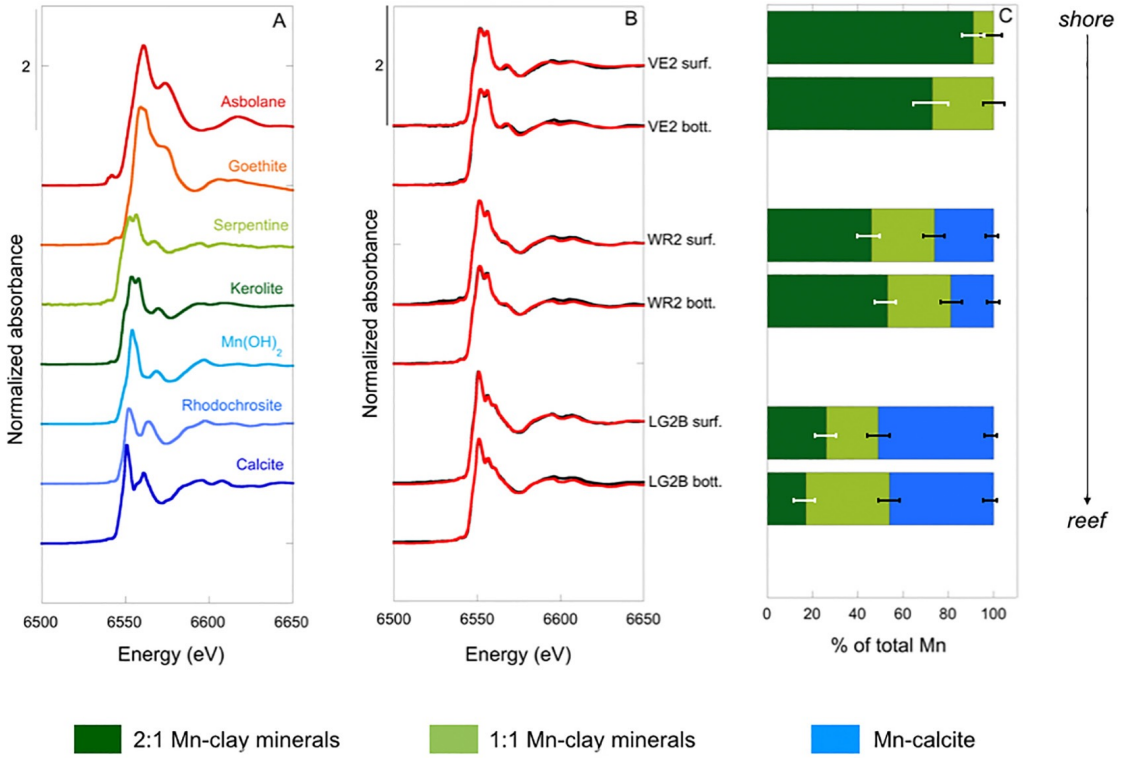

Fig. 5. Mn K-edge XANES spectra of (A) the model compounds used for the LC-LSF analysis and (B) the lagoon sediment samples (experimental data in black and LC- LS fits in red). The quantitative results of the LC-LS fits on Mn speciation are shown in (c). Surface samples correspond to 1–2 cm depth for the three cores. Bottom samples correspond to 16.5–17.5 cm depth for core VE2, 19.5–20.5 cm depth for core WR2 and 17.5–18.5 cm depth for core LG2B. (For interpretation of the references to colour in this figure legend, the reader is referred to the web version of this article.)

Concerning Cr redox state, the pre-edge region of the normalized Cr K-edge XANES spectra from the studied sediments showed two peaks at 5990 and 5993 eV that could be related to Cr(III) and Cr(VI), respec- tively (Fig. 4). When normalized to the intensity of the pre-edge peak at 5990 eV, comparison with the pre-edge peaks from synthetic mixture containing either 0% or 5% Cr(VI) suggested that the studied sediments could hold a small fraction of Cr(VI) (Fig. 4). Moreover, this fraction of Cr(VI) that would not exceed 2–3% of total Cr would increase from the shore to the reef since the intensity of the pre-edge peak at 5994 eV show a regular increase across this gradient (Fig. 4).

However, detailed comparison of the pre-edge peaks from the stud- ied sediments with those of the model compounds used in the LC-LS fits lead to mitigate these assumptions. Especially, although it contains no Cr(VI), the pre-edge region of the Cr K-edge XANES spectrum of Cr(III)-bearing goethite shows a strong peak at 5994 eV (Fig. 4). This increased intensity of the pre-edge peak at 5993 eV is due to a loss of symmetry of the octahedral site of Cr(III), which results from structural distortion because of the difference in ionic radius between Fe(III) and Cr(III) (Fandeur et al., 2009a). The increasing intensity of the pre-edge peak at 5994 eV observed on the Cr Kedge XANES spectra from the studied sediments across the shore-to-reef gradient is thus likely to be due to the increasing fraction of Cr(III)-bearing

goethite across this gradient as indicated by the LC-LS fits (Fig. 3; Table S6). Considering the accuracy of this approach based on intensity of the XANES pre-edge peaks (Fandeur et al., 2009a), these latter results lead to rule out the possible occurrence of Cr(VI) in the studied sediments.

3.4. XAS-derived Mn speciation

PCA analysis of the Mn K-edge XANES spectra of the 6 sediment samples suggested that 3 components were necessary to reconstruct the experimental data set (Fig. S2). The results of the TT analysis showed that Mn-bearing clay minerals (*i.e.* serpentine and kerolite), Mn-bearing olivine, Mn-bearing vivianite, Mn-bearing siderite, Mn-bearing calcite and rhodochrosite had the lowest Chi^2 values (Table S7) and were consequently the most relevant model compounds to be used for the LS- LCF procedure. In contrast, Mn(IV)-oxides and Mn-bearing goethite exhibited high Chi^2 values and were thus ranked as less relevant (Fig. 5; Table S7). The Mn-bearing serpentine model compound (Fig. 5; Table S7) was considered as a relevant proxy for Mn impurities in 1/1 clay minerals (*i.e.* chrysotile and greenalite/berthierine), in agreement with TEM-EDXS observations (Fig. S3 and Merrot et al., 2019). In the same way, the Mn-bearing kerolite model compound was considered as a possible proxy for Mn incorporated in the octahedral layer of 2/1 clay minerals (*i.e.* Fe-rich smectite) that have also been identified by TEM- EDXS (Fig. S3 and Merrot et al., 2019). Finally, regarding the low Chi^2 value returned by the TT analysis (Fig. 5; Table S7), the Mn-bearing calcite model compound was considered as a good candidate for Mn incorporated in the Mg-calcite and calcite, which is also supported by the large occurrence of these carbonate minerals in the same sediment samples, especially near the coral reef (Fig. S1; Merrot et al., 2019). Although the TT analysis also returned a low Chi^2 value for rhodo- chosite, this model compound did not match the Mn K-edge XANES data of the sediment samples, when included as a fitting component.

The best LC-LS fits of the normalized Mn K-edge XANES spectra were obtained by using Mn-bearing kerolite, Mn-bearing serpentine and Mn- bearing calcite as fitting components. These results showed that Mn- bearing clay minerals are the only Mn-hosts in the sediments close to the shore (Fig. 5; Table S8). However, this contribution progressively decreases towards the coral reef, where it becomes similar to that of Mn- bearing calcite (Fig. 5; Table S8). Within the Mn-bearing clay minerals pool, the 2/1 clay minerals dominate over the 1/1 clay minerals close to the shore (*i.e.* 74–94% compared to 9–28% of Mn speciation; Fig. 5; Table S8), whereas the 1/1 clay minerals become dominant over the 2/1 clay minerals close to the coral reef (*i.e.* 24–36% of Mn speciation compared to 17–27% of Mn speciation; Fig. 5; Table S8). The contri- bution of Mn-bearing carbonate species is not detectable in the sedi- ments close to the shore, but it significantly increases across the shore- to-reef gradient to reach 45–54% of Mn speciation in the sediments close to the coral reef (Fig. 5; Table S8). This evolution of Mn speciation reflects the dramatic change from silicate to carbonate mineral species observed in the mineralogy of the studied sediments across the shore-to- reef gradient (Fig. S1; Merrot et al., 2019).

4. Discussion

4.1. Continental vs. marine Mn host phases

Our Mn K-edge XAS data indicate that Mn is only incorporated in clay minerals in the sediments close to the shore (Fig. 5; Table S8), in which the mineralogy is dominated by silicate minerals (Fig. S1; Merrot et al., 2019). In these sediments, Mn speciation is dominated by 2/1 clay minerals. However, this contribution decreases across the shore-to-reef gradient, whereas that of 1/1 clay minerals slightly increases. This contrasted evolution between these two types of clay minerals in the studied lagoon sediments could indicate different sources. Regarding its decreasing contribution to Mn speciation from the shore to the reef (Fig. 5; Table S8), the Fe-rich 2/1 clay minerals of the smectite/non- tronite family

detected by TEM-EDXS likely derive from continental input. The detection of the same type of clay minerals just upstream in the mangrove sediments of the Vavouto Bay (No¨el et al., 2014) strongly supports this hypothesis. In addition, the lack of detection of these clay minerals in the Ferralsols of the Koniambo lateritic regolith (Dublet et al., 2012, 2017) lead No¨el et al. (2014) to suggest that it could have formed in the mangrove sediments. Consequently, the Fe-rich 2/1 clay minerals of the smectite/nontronite family detected by TEM-EDXS in the studied lagoon sediments are considered to originate from the upstream mangrove sediments. On the opposite, the detection of Mn-bearing 1/1 clay minerals in the Ferralsols of the Koniambo lateritic regolith (Dublet et al., 2017) suggests that the Mn-bearing chrysotile identified by TEM- EDXS in the studied lagoon sediments (Fig. S3) could be inherited from lateritic inputs. However, the slight increase of the contribution of 1/1 clay minerals to Mn speciation across the shore-to-reef gradient (Table S8) also supports the hypothesis of an *in-situ* formation in the studied lagoon sediments. This *in-situ* formation would especially concern the Mn-bearing greenalite/berthierine, as already proposed by Merrot et al. (2019). In addition to clay minerals, Mn K-edge XAS data also indicate an increasing contribution of Mn-bearing calcite to Mn speciation from the shore to the reef (Fig. 5; Table S8). Despite the well- known capacity of Mn to structurally incorporate in calcite through Mn (II) for Ca(II) isomorphous substitution and thus to accumulate in ma- rine sediments as Mn-bearing calcite (Paquette and Reeder, 1995; Bo¨ttcher, 1998; Bamforth et al., 2006; Soldati et al., 2016; Barras et al., 2018; Son et al., 2019), it is important to note here that the Mn-bearing calcite model compounds used for LC-LSF quantitative analyses of Mn K- edge XAS data has to be considered as a proxy for Mn-bearing carbonate minerals. Indeed, a recent XAS study on a set of carbonated sedimentary Mn deposits ranging from modern to 2 billion years old reported kut- nohorite ($CaMn(CO_3)_2$) and rhodochrosite ($MnCO_3$) as the major Mn- hosts in ancient marine sedimentary settings (Johnson et al., 2016). Although our Mn K-edge XANES data allow to dismiss rhodochrosite as a candidate for Mn speciation in the studied lagoon sediments, the possible occurrence of kutnohorite instead of, or together with, Mn- bearing calcite cannot be ruled out because of the very similar Mn K- edge XANES spectra between both mineral phases (Fig. 5; Johnson et al., 2016). Following this interpretation, it is better to consider that the LC- LS fits of our Mn K-edge XANES data show an increasing contribution of Mn-bearing carbonate minerals, rather than Mn-bearing calcite, to Mn speciation from the shore to the reef (Fig. 5; Table S8). Since this trend can be directly linked to the similar increasing fraction of Ca/Mg car- bonate minerals revealed by XRD (Fig. S1), the contribution of the Mn- bearing carbonate minerals to Mn speciation quantified in the studied lagoon sediments can be related to a marine Mn source. Regarding the expected continental origin for Ti, this hypothesis is supported by the increase of the Mn/Ti ratio as a function of the Ca content that can be observed across the shore-to-reef gradient (Fig. S4). All the above results thus strongly suggest a mixed sourcing for Mn-bearing mineral phases in the studied lagoon sediments, with Fe-rich smectite/nontronite and chrysotile of continental origin, Ca/Mg-carbonates of marine origin and authigenic greenalite/berthierine.

4.2. Ultramafic origin of the Cr-host phases

Our Cr K-edge XAS data indicate that the major Cr host in the lagoon sediments close to the shore is chromite (Fig. 3; Tables S6). This mineral is the principal Cr host in the Ferralsols of the Koniambo lateritic regolith, where it is inherited from the ultramafic bedrocks (*i.e.* peri- dotites; Fandeur et al., 2009b). Chromite is thus considered to have deposited in the lagoon sediments of the Vavouto Bay after erosion of the Koniambo lateritic regolith (Fig. 1). This hypothesis is consistent with the already reported occurrence of detrital chromite in coastal sediments downstream of ultramafic (Prego et al., 2014; Ergin et al., 2007) and basaltic (Gujar et al., 2010) continental settings. In addition to chromite, our Cr K-edge XAS data also indicate a significant contribution of Cr- bearing clay minerals to Cr speciation in the lagoon sediments close to the shore (Table S6). The progressive decrease of this contribution to- wards the coral reef suggests a continental source for the Cr-bearing clay minerals found in the studied sediments. This hypothesis is supported by the reported occurrence of Cr-bearing clay minerals such as chrysotile in

the Koniambo regolith, especially in the saprolite unit (Fandeur et al., 2009b). Such an occurrence of Cr-bearing clay minerals in both the Koniambo lateritic regolith and the downstream lagoon sediments is supported by the well-known affinity of Cr(III) ions for the octahedral layers of clay minerals (Zampella et al., 2010; Bianchini et al., 2002; Gan, 1996). Finally, our Cr K-edge XAS data indicate a small contribu- tion of Cr-bearing goethite to Cr speciation in the lagoon sediments close to the shore (Table S6). This result would be in agreement with the continental input of Cr-bearing goethite in the Ferralsols at the top of the Koniambo lateritic regolith (Dublet et al., 2012, 2015; Fandeur et al., 2009a,b). Chromite, Cr-bearing goethite and Cr-bearing clay minerals thus appear as the major Cr hosts in the studied lagoon sediments (Fig. 3) and the reported occurrence of these mineral phases in the Ferralsols of the Koniambo lateritic regolith (Dublet et al., 2015; Fan- deur et al., 2009a,b) strongly supports the hypothesis of their major sourcing from this geological setting.

4.3. Lack of detectable Cr(VI) and absence of Mn-oxides

Owing to their strong capacity to oxidize Cr(III) (Apte et al., 2006; Motzer, 2005; Kim et al., 2002b; Koˇzuh et al., 2000; Nico and Zasoski, 2000; Banerjee and Nesbitt, 1999; Fendorf et al., 1992; Manceau and Charlet, 1992), Mn(IV)-oxides are considered as the main driver for the potential occurrence of Cr(VI) in the studied lagoon sediments. As a consequence, the absence of Mn(IV)-oxides revealed by Mn K-edge XANES data likely explains the lack of Cr(VI) detection by Cr K-edge XANES data. This absence of Mn(IV)-oxides in the lagoon sediments downstream of the Koniambo lateritic regolith is surprising since these mineral phases have been identified as an important Mn host in the Koniambo lateritic regolith, especially in the transition lateritic unit (Fandeur et al., 2009a; Dublet et al., 2017). As a first hypothesis to explain this apparent discrepancy, the Mn(IV)-oxides inherited from the Koniambo lateritic regolith could have been reductively dissolved in the mangrove sediments, which represent an intermediate depositional environment between the Koniambo lateritic regolith and the lagoon sediments. This first hypothesis relies on the results of studies that re- ported the occurrence of Mn(IV)-oxides in mangrove sediments and showed that these Mn mineral phases undergo reductive dissolution within the euxinic conditions of these sedimentary settings (Noronha- D'Mello and Nayak, 2015; Kumar and Ramanathan, 2015; Marchand et al., 2012; Jingchun et al., 2006). In contrast to Fe(II) that has been largely shown to precipitate as Fe-sulfides after reaction with aqueous sulfides in mangrove sediments (Huerta-Diaz and Morse, 1992; Wang and Morse, 1996, Morse and Wang, 1997, Neretin et al., 2004, Li et al., 2006; No¨el et al., 2014, 2015), reported occurrences of Mn-sulfides in euxinic sedimentary settings are scarce and they are associated with low Fe(II) conditions (Bo¨ttcher and Huckriede, 1997; Lepland and Stevens, 1998; Lenz et al., 2014). In the Fe-rich mangrove sediments downstream of the Koniambo lateritic regolith (No¨el et al., 2014, 2015), Mn(II) released from Mn(IV)-oxides reductive dissolution would thus be ex- pected to precipitate as carbonate minerals (Otero et al., 2009; Lenz et al., 2014; Johnson et al., 2016) or to complex with dissolved organic matter and remain in the pore water (Marchand et al., 2012). In addition to this first hypothesis, the marked decrease of the Mn concentration within the first centimeters of the sediments close to the shore (VE2; Fig. 2) also suggests that the Mn(IV)-oxides possibly inherited from the Koniambo lateritic regolith could have reductively dissolved *in-situ*. This second hypothesis is supported by the anoxic character of the studied lagoon sediments below 5 mm depth reported by O_2 micro-profiling measurements (Merrot et al., 2019). In such anoxic conditions that are driven by the biological degradation of organic matter (Froelich et al., 1978; Berner, 1980; Stumm and Morgan, 1996; Slomp et al., 1997), any inherited Mn(IV)-oxides would indeed have been reduced within the first top centimeters of the sediments (Shaw et al., 1990; Burdige, 1993; Canfield et al., 1993; Davison, 1993; Thamdrup et al., 1994; Wang and Van Cappellen, 1996; Slomp et al., 1997). The lack of detection of Mn (IV)-oxides in the lagoon sediments of the Vavouto Bay can thus be explained by the hypotheses that any fraction of these mineral phases that would have been inherited from the Koniambo lateritic regolith would have reductively dissolved, either in the euxinic mangrove sedi- ments before being further transported towards the lagoon environment, or *in-situ* in the lagoon sediments close to the

shore because of the anoxic conditions that develop after complete oxygen consumption within the first centimeters depth (Merrot et al., 2019).

4.4. Evolution of the Cr-host phases in the lagoon sediments

As already mentioned, our Cr K-edge XAS data indicate that Cr oc- curs as chromite, Cr(III)-bearing clay minerals and Cr(III)-bearing goethite in the studied sediments, and the absence of Mn-oxides sup- ported by Mn K-edge XAS data suggests that oxidation of Cr(III) to Cr(VI) is unlikely. The high Cr concentration in the sediments from the Vavouto Bay (Fig. 2; Table S3) should thus not represent a significant hazard. Besides, our Cr K-edge XAS results also show that the contributions of chromite and clay minerals to Cr speciation decrease from the shore to the reef, whereas that of goethite increases (Fig. 3; Table S6). In parallel, the contribution of clay minerals to Cr speciation also decreases, but to a lesser extent that is close to the uncertainty of the LC-LSF analysis (Fig. 3; Table S6). These trends suggest that chromite and clay minerals could have weathered and partially transformed into Cr-bearing goethite during their transport from the shore to the reef. However, such a possible weathering of clay minerals from the shore to the reef would be inconsistent with the results of Merrot et al. (2019), which showed an increasing contribution of clay minerals to Fe speciation across this gradient. This latter finding was interpreted as an evidence that both detrital serpentines and authigenic green-clays represent long- term sink for iron in the studied lagoon sediments. Concerning chromite that is generally considered as a resistant mineral (Stanin, 2005; Schmidt, 1984), several studies have reported a partial weathering and incongruent dissolution of this mineral species during intense lateriti- zation processes such as those that produced the thick lateritic regoliths in New Caledonia. For instance, Fandeur et al. (2009b) have shown that $(Fe,Mg)(Cr,Al)_2O_4$ chromite inherited from the peridotites bedrock could be progressively weathered into $FeCr_2O_4$ that ultimately trans- formed into Cr bearing goethite α-(Fe,Cr)OOH, the two latter minerals forming concentric rims surrounding the pristine chromite grains. This preferential leaching of Mg and Al from chromite that would leave a Fe/ Cr-rich residue upon weathering has previously been proposed to explain the occurrence of two populations of chromite in serpentinite soils from California-USA (Oze et al., 2004) and Ferralsols from Niquelaˆndia-Brazil (Garnier et al., 2008). It was also in agreement with the results reported for the experimental weathering of chromite from the Bushweld complex (Merkle et al., 2004). These previous studies suggest thus that Cr(III)-bearing goethite can form after chromite weathering. Such a formation of Cr-bearing goethite after chromite is supported by the Cr(III) for Fe(III) isomorphic substitution in goethite (*i. e.* up to 1.6 mol% CrOOH) already reported for both synthetic and natural samples (Stipp et al., 2002; Manceau et al., 2000; Trolard et al., 1995; Bidoglio et al., 1993), and typically encountered in Ferralsols and lateritic regoliths from New Caledonia (Becquer et al., 2003; Fandeur et al., 2009a,b). In the sedimentary context of the Vavouto Bay, this process could have been triggered either during sediments transport from the shore to the reef or upon re-suspension of surface sediments due to the strong currents that are especially generated close to the reef pass. These two situations that would have caused the sediments to be suspended in oxygenated waters would have indeed favored the Fe(II) to Fe(III) oxidation that is necessary to drive chromite transformation into Cr(III)-bearing goethite. In addition, despite the low solubility of Cr(III) species, dissolved organic carbon could have favored chromite dissolu- tion *via* the formation of organo-Cr(III) complexes (James and Bartlett, 1983; Richard and Bourg, 1991; Fendorf, 1995; Puzon et al., 2005, 2008; Gustafsson et al., 2014; Fan et al., 2019). Altogether, these consider- ations suggest that a fraction of Cr could have been released towards the water column due to chromite weathering into goethite, which could explain the decrease of the Cr/Ti ratios when approaching the coral reef (Fig. S4). Besides this putative process, size sorting during particle transport from the shore to the reef could also partly explain the decrease of the chromite contribution to Cr speciation, since this latter mineral has been shown to exhibit larger particle sizes than goethite in lateritic regoliths from New Caledonia (Fandeur et al., 2009a,b). Indeed, the increase in clay size-fraction observed from the shore to the reef (Table S2) would be consistent with the preferential transport of goethite over chromite across this gradient. Hence, the Cr depletion and the increase of the goethite contribution to Cr speciation that are observed across the shore-to-reef gradient in the studied

lagoon sedi- ments could be explained by both chromite weathering into Cr(III)- bearing goethite and sediments granulometric sorting. Consequently, Cr-bearing goethite appears as the major form of Cr expected to be transported in the solid fraction from the lagoon sediments to the ocean. Further studies should however be engaged in order to better quantify the suspected Cr release towards the water column upon chromite weathering across the shore-to-reef gradient and to test the hypothesis of a Cr flux at the sediment/water interface through the formation of organo-Cr(III) complexes upon early diagenesis.

CRediT authorship contribution statement

Pauline Merrot: Conceptualization, Investigations, Formal analysis, Writing original draft, Writing, review and editing. **Farid Juillot**: Project administrator and funding acquisition, Conceptualization, Investigation, Formal analysis, Writing, review and editing. **Pierre Le Pape**: Conceptualization, Investigations, Formal analysis, Writing, re- view and editing. **Pierre Lefebvre**: Investigations. **Jessica Brest**: In- vestigations. **Isabelle Kieffer**: Investigations. **Nicolas Menguy**: Investigations. **Eric Viollier**: Conceptualization, Investigation, Formal analysis, Writing, review and editing. **Jean-Michel Fernandez**: Conceptualization, Investigation, Formal analysis, Writing, review and editing. **Benjamin Moreton**: Conceptualization, Investigation, Formal analysis, Writing, review and editing. **Olivier radakovitch**: Investiga- tion, Formal analysis, Writing, review and editing. **Guillaume Morin**: Conceptualization, Investigation, Formal analysis, Writing, review and editing.

Declaration of competing interest

The authors declare no conflict of interest.

Acknowledgements

The technical staff at the FAME beamline of the European Synchro- tron Radiation Facility (ESRF, Grenoble, France), the SAMBA beamline at the Source Optimis´ee de Lumi`ere d'Energie Interm´ediaire du LURE synchrotron (SOLEIL, Saint-Aubin, France) and the XAFS beamline at Elettra Synchrotron (Trieste, Italy) are greatly acknowledged for providing good beamtime conditions. Thanks are extended to Jean-Michel Guigner (IMPMC, Paris, France) for help during TEM-EDXS an- alyses and to the technical staff at Laboratoire des Moyens Analytiques (LAMA-IMAGO) of the IRD Center in Noumea (New Caledonia) for ICP- OES analyses. A part of this study was funded by the CNRT (Centre National de Recherche Technologique sur le nickel et son environne- ment - www.cnrt.nc) through the DYNAMINE project (2015–2018).

Appendix A. Supplementary data

Supplementary data to this article can be found online at https://doi. org/10.1016/j.gexplo.2021.106845.

References

Ambatsian, P., Fernex, F., Bernat, M., Parron, C., Lecolle, J., 1997. High metal inputs to closed seas: the New Caledonian lagoon. J. Geochem. Explor. 59, 59–74. https://doi. org/10.1016/S0375-6742(96)00020-9.

Apte, A., Tare, V., Bose, P., 2006. Extent of oxidation of Cr(III) to Cr(VI) under various conditions pertaining to natural environment. J. Hazard. Mater. 128, 164–174. https://doi.org/10.1016/j.jhazmat.2005.07.057.

Bamforth, S.M., Manning, D.A.C., Singleton, I., Younger, P.L., Johnson, K.L., 2006. Manganese removal from mine waters – investigating the occurrence and importance of manganese carbonates. Appl. Geochem. 21, 1274–1287. https://doi. org/10.1016/j.apgeochem.2006.06.004.

Banerjee, D., Nesbitt, H.W., 1999. Oxidation of aqueous Cr(III) at birnessite surfaces: constraints on reaction mechanism. Geochim. Cosmochim. Acta 63, 1671–1687. https://doi.org/10.1016/S0016-7037(99)00003-4.

Bargar, J.R., Tebo, B.M., Bergmann, U., Webb, S.M., Glatzel, P., Chiu, V.Q.,Villalobos, M., 2005. Biotic and abiotic products of Mn(II) oxidation by spores of the marine Bacillus sp. strain SG-1. Am. Mineral. 90, 143–154. https://doi.org/10.2138/ am.2005.1557.

Barras, C., Mouret, A., Nardelli, M.P., Metzger, E., Petersen, J., La, C., Filipsson, H.L., Jorissen, F., 2018. Experimental calibration of manganese incorporation in foraminiferal calcite. Geochim. Cosmochim. Acta 237, 49–64. https://doi.org/ 10.1016/j.gca.2018.06.009.

Becquer, T., Quantin, C., Sicot, M., Boudot, J.P., 2003. Chromium availability in ultramafic soils from New Caledonia. Sci. Total Environ. 301, 251–261.

Becquer, T., Quantin, C., Rotte-Capet, S., Ghanbaja, J., Mustin, C., Herbillon, A.J., 2006. Sources of trace metals in Ferralsols in New Caledonia. Eur. J. Soil Sci. 57, 200–213. https://doi.org/10.1111/j.1365-2389.2005.00730.x.

Berner, R.A., 1980. Early Diagenesis: A Theoretical Approach. Princeton University Press, New Jersey.

Bianchini, G., Laviano, R., Lovo, S., Vaccaro, C., 2002. Chemical–mineralogical characterisation of clay sediments around Ferrara (Italy): a tool for an environmental analysis. Appl. Clay Sci. 21, 165–176. https://doi.org/10.1016/S0169-1317(01) 00086-2.

Bidoglio, G., Gibson, P.N., O'Gorman, M., Roberts, K.J., 1993. X-ray absorption spectroscopy investigation of surface redox transformations of thallium and chromium on colloidal mineral oxides. Geochim. Cosmochim. Acta 57, 2389–2394. https://doi.org/10.1016/0016-7037(93)90576-I.

Bishop, M.E., Dong, H., Glasser, P., Briggs, B.R., Pentrak, M., Stucki, J.W., Boyanov, M.I., Kemner, K.M., Kovarik, L., 2014. Reactivity of redox cycled Fe-bearing subsurface sediments towards hexavalent chromium reduction. Geochim. Cosmochim. Acta 252, 88–106. https://doi.org/10.1016/j.gca.2019.02.039.

Bishop, M.E., Dong, H., Glasser, P., Briggs, B.R., Pentrak, M., Stucki, J.W., Boyanov, M.I., Kemner, K.M., Kovarik, L., 2019. Reactivity of redox cycled Fe-bearing subsurface sediments towards hexavalent chromium reduction. Geochim. Cosmochim. Acta 252, 88–106. https://doi.org/10.1016/j.gca.2019.02.039.

Bo¨ttcher, M.E., 1998. Manganese(II) partitioning during experimental precipitation of rhodochrosite-calcite solid solutions from aqueous solutions. Mar. Chem. 62, 287–297. https://doi.org/10.1016/S0304-4203(98)00039-5.

Bo¨ttcher, M.E., Huckriede, H., 1997. First occurrence and stable isotope composition of authigenic γ-MnS in the central Gotland Deep (Baltic Sea). Mar. Geol. 137, 201–205. https://doi.org/10.1016/S0025-3227(96)00115-6.

Burdige, D.J., 1993. The biogeochemistry of manganese and iron reduction in marine sediments. Earth Sci. Rev. 35, 249–284. https://doi.org/10.1016/0012-8252(93) 90040-E.

Burt, R., Wilson, M.A., Mays, M.D., Lee, C.W., 2003. Major and trace elements of selected pedons in the USA. J. Environ. Qual. 32, 2109. https://doi.org/10.2134/ jeq2003.2109.

Canfield, D.E., Thamdrup, B., Hansen, J.W., 1993. The anaerobic degradation of organic matter in Danish coastal sediments: iron reduction, manganese reduction, and sulfate reduction. Geochim. Cosmochim. Acta 57, 3867–3883. https://doi.org/ 10.1016/0016-7037(93)90340-3.

Dalto, A.G., Gr´emare, A., Dinet, A., Fichet, D., 2006. Muddy-bottom meiofauna responses to metal concentrations and organic enrichment in New Caledonia South-West Lagoon. Estuar. Coast. Shelf Sci. 67, 629–644. https://doi.org/10.1016/j. ecss.2006.01.002.

Davison, W., 1993. Iron and manganese in lakes. Earth Sci. Rev. 34, 119–163. https:// doi.org/10.1016/0012-8252(93)90029-7.

Doyle, C.S., Kendelewicz, T., Bostick, B.C., Brown, G.E., 2004. Soft X-ray spectroscopic studies of the reaction of fractured pyrite surfaces with Cr(VI)-containing aqueous

solutions. Geochim. Cosmochim. Acta 68, 4287–4299. https://doi.org/10.1016/j.

gca.2004.02.015.Dublet, G., Juillot, F., Morin, G., Fritsch, E., Fandeur, D., Ona-Nguema, G., Brown, G.E.,

2012. Ni speciation in a New Caledonian lateritic regolith: a quantitative X-ray absorption spectroscopy investigation. Geochim. Cosmochim. Acta 95, 119–133. https://doi.org/10.1016/j.gca.2012.07.030.

Dublet, G., Juillot, F., Morin, G., Fritsc, E., Fandeur, D., Brown, G.E., 2015. Goethite aging explains Ni depletion in upper units of ultramafic

lateritic ores from New Caledonia. Geochim. Cosmochim. Acta 160, 1–15. https://doi.org/10.1016/j. gca.2015.03.015.

Dublet, G., Juillot, F., Brest, J., No¨el, V., Fritsch, E., Proux, O., Oliv, L., Ploquin, F., Morin, G., 2017. Vertical changes of the Co and Mn speciation along a lateritic regolith developed on peridotites (New Caledonia). Geochim. Cosmochim. Acta 217, 1–15. https://doi.org/10.1016/j.gca.2017.07.010.

Eary, L.E., Rai, D., 1987. Kinetics of chromium(III) oxidation to chromium(VI) by reaction with manganese-dioxide. Environ. Sci. Technol. 21, 1187–1193. https:// doi.org/10.1021/es00165a005.

Ergin, M., Keskin, S¸., Dog˘an, A.U., Kadıog˘lu, Y.K., Karaka, Z., 2007. Grain size and heavy mineral distribution as related to hinterland and environmental conditions for modern beach sediments from the Gulfs of Antalya and Finike, eastern Mediterranean. Mar. Geol. 240, 185–196. https://doi.org/10.1016/j. margeo.2007.02.006.

Fan, X., Ding, S., Chen, M., Gao, S., Fu, Z., Gong, M., Tsang, D.C.W., Wang, Y., Zhang, C., 2019. Peak chromium pollution in summer and winter caused by high mobility of chromium in sediment of a eutrophic lake: in situ evidence from high spatiotemporal sampling. Environ. Sci. Technol. 53, 4755–4764. https://doi.org/10.1021/acs. est.8b07060.

Fandeur, D., Juillot, F., Morin, G., Olivi, L., Cognigni, A., Webb, S.M., Ambrosi, J.-P., Fritsch, E., Guyot, F., Brown Jr., G.E., 2009a. XANES evidence for oxidation of Cr(III) to Cr(VI) by Mn-oxides in a lateritic regolith developed on serpentinized ultramafic rocks of New Caledonia. Environ. Sci. Technol. 43, 7384–7390. https://doi.org/ 10.1021/es900498r.

Fandeur, D., Juillo, F., Morin, G., Olivi, L., Cognign, A., Ambrosi, J.-P., Guyot, F., Fritsch, E., 2009b. Synchrotron-based speciation of chromium in an oxisol from New Caledonia: Importance of secondary Fe-oxyhydroxides. Am. Miner. 94, 710–719. https://doi.org/10.2138/am.2009.3073.

Fendorf, S.E., 1995. Surface reaction of chromium in soils and waters. Geoderma 67, 55–71. https://doi.org/10.1016/0016-7061(94)00062-F.

Fendorf, S.E., Li, G., 1996. Kinetics of chromate reduction by ferrous iron. Environ. Sci. Technol. 30, 1614–1617. https://doi.org/10.1021/es950618m.

Fendorf, S.E., Fendorf, M., Sparks, D.L., Gronsky, R., 1992. Inhibitory mechanisms of Cr (lll) oxidation by ∂-Mn0_2. J. Colloid Interface Sci. 153, 37–54. https://doi.org/ 10.1016/0021-9797(92)90296-X.

Feng, X.H., Zhai, L.M., Tan, W.F., Liu, F., He, J.Z., 2007. Adsorption and redox reactions of heavy metals on synthesized Mn oxide minerals. Environ. Pollut. 147, 366–373. https://doi.org/10.1016/j.envpol.2006.05.028.

Fritsch, E., 2012. Les sols. In: Bonvallot, J., Gay, J.-C., Habert, E. (Eds.), Atlas de la Nouvelle-Cal´edonie. IRD & Congr`es de la Nouvelle-Cal´edonie, Marseille.

Froelich, P.N., Klinkhammer, G.P., Bender, M.L., Luedtke, N.A., Heath, G.R., Cullen, D., Dauphin, P., Hammond, Blaynehartman D., 1978. Early oxidation of organic matter in pelagic sediments of the eastern equatorial Atlantic: suhoxic diagenesis. Geochim. Cosmochim. Acta 43, 1075–1090. https://doi.org/10.1016/0016-7037(79)90095-4.

Gan, H., 1996. Morphology of lead(II) and chromium(III) reaction products on phyllosilicate surfaces as determined by atomic force microscopy. Clay Clay Miner. 44, 734–743. https://doi.org/10.1346/CCMN.1996.0440603.

Garnier, J., Quantin, C., Guimaraes, E., Becquer, T., 2008. Can chromite weathering be a source of Cr in soils? Mineral. Mag. 72, 49–53. https://doi.org/10.1180/ minmag.2008.072.1.49.

Gaudry, E., Cabaret, D., Brouder, C., Letard, I., Rogalev, A., Wilhlem, F., Jaouen, N., Sainctavit, P., 2007. Relaxations around the substitutional chromium site in emerald: X-ray absorption experiments and density functional calculations. Phys. Rev. B 76, 094110. https://doi.org/10.1103/PhysRevB.76.094110.

Guertin, J., 2005. Toxicity and health effects of chronium (all oxidation states). In: Guertin, J., Jacobs, J.A., Avakian, C. (Eds.), Chromium (VI) Handbook. CRC Press, Boca Raton, Fla., pp. 215–234

Gujar, A.R., Ambre, N.V., Mislankar, P.G., Iye, S.D., 2010. Ilmenite, magnetite and chromite beach placers from South Maharashtra, Central West Coast of India. Resour. Geol. 60, 71–86. https://doi.org/10.1111/j.1751-3928.2010.00115.x.

Gustafsson, J.P., Persson, I., Oromieh, A.G., van Schaik, J.W.J., Sjostedt, C., Kleja, D.B., 2014. Chromium(III) complexation to natural organic matter: mechanisms and modeling. Environ. Sci. Technol. 48, 1753–1761. https://doi.org/10.1021/ es404557e.

He, Y.T., Traina, S.J., 2005. Cr(VI) reduction and immobilization by magnetite under alkaline pH conditions: the role of passivation. Environ. Sci. Technol. 39, 4499–4504. https://doi.org/10.1021/es0483692.

Huerta-Diaz, M.A., Morse, J.W., 1992. Pyritization of trace metals in anoxic marine sediments. Geochim. Cosmochim. Acta 56, 2681–2702. https://doi.org/10.1016/ 0016-7037(92)90353-K.

Huggins, F.E., Najih, M., Huffman, G.P., 1999. Direct speciation of chromium in coal combustion by-products by X-ray absorption fine-structure spectroscopy. Fuel 78, 233–242. https://doi.org/10.1016/S0016-2361(98)00142-2.

Jacobs, J.A., Testa, S.M., 2005. Overview of chromium(VI) in the environment: background and history. In: Guertin, J., Jacobs, J.A., Avakian, C. (Eds.), Chromium (VI) Handbook. CRC Press, Boca Raton, Fla., pp. 1–21

James, B.R., Bartlett, R.LJ., 1983. Behavior of chromium in soils: VII. Adsorption and reduction of hexavalent forms. J. Environ. Qual. 12, 177–181.

Jingchun, L., Chongling, Y., Macnair, M.R., Jun, H., Yuhong, L., 2006. Distribution and speciation of some metals in mangrove sediments from Jiulong River estuary, People's Republic of China. Bull. Environ. Contamin. Toxicol. 76, 815–822. https:// doi.org/10.1007/s00128-006-0992-0.

Joe-Wong, C., Brown Jr., G.E., Maher, K., 2017. Kinetics and products of chromium (VI) reduction by iron (II/III)-bearing clay minerals. Environ. Sci. Technol. 51, 9817–9825. https://doi.org/10.1021/acs.est.7b02934.

Johnson, J.E., Webb, S.M., Ma, C., Fischer, W.W., 2016. Manganese mineralogy and diagenesis in the sedimentary rock record. Geochim. Cosmochim. Acta 173, 210–231. https://doi.org/10.1016/j.gca.2015.10.027.

Juhin, A., Brouder, C., Arrio, M.-A., Cabaret, D., Sainctavit, P., Balan, E., Bordage, A., Seitsonen, A.P., Calas, G., Eeckhout, S.G., Glatzel, P., 2008. X-ray linear dichroism in cubic compounds: the case of Cr 3 + in MgAl 2 O 4. Phys. Rev. B 78, 195103. https://doi.org/10.1103/PhysRevB.78.195103.

Kendelewicz, T., Liu, P., Doyle, C.S., Brown, G.E., 2000. Spectroscopic study of the reaction of aqueous Cr(VI) with Fe3O4 (111) surfaces. Surf. Sci. 469, 144–163. https://doi.org/10.1016/S0039-6028(00)00808-6.

Kim, J., Jung, P.-K., Moon, H.-S., Chon, C.-M., 2002b. Reduction of hexavalent chromium by pyrite-rich andesite in different anionic solutions. Environ. Geol. 42, 642–648. https://doi.org/10.1007/s00254-002-0567-2.

Kim, J.G., Dixon, J.B., Chusuei, C.C., Deng, Y., 2002a. Oxidation of chromium(III) to (VI) by manganese oxides. Soil Sci. Soc. Am. J. 66, 306–315. https://doi.org/10.2136/ sssaj2002.0306.

Koˇzuh, N., Sˇtupar, J., Gorenc, B., 2000. Reduction and oxidation processes of chromium in soils. Environ. Sci. Technol. 34, 112–119. https://doi.org/10.1021/es981162m. Kumar, A., Ramanathan, A., 2015. Speciation of selected trace metals (Fe, Mn, Cu and

Zn) with depth in the sediments of Sundarban mangroves: India and Bangladesh.

J. Soils Sediments 15, 2476–2486. https://doi.org/10.1007/s11368-015-1257-5. Landrot, G., Ginder-Vogel, M., Sparks, D.L., 2010. Kinetics of chromium(III) oxidation by

manganese(IV) oxides using quick scanning X-ray absorption fine structure spectroscopy (Q-XAFS). Environ. Sci. Technol. 44, 143–149. https://doi.org/ 10.1021/es901759w.

Landrot, G., Ginder-Vogel, M., Livi, K., Fitts, J.P., Sparks, D.L., 2012. Chromium(III) oxidation by three poorly-crystalline manganese-(IV) oxides. 1. Chromium(III)- oxidizing capacity. Environ. Sci. Technol. 46, 11594–11600. https://doi.org/ 10.1021/es302383y.

Lenz, C., Behrends, T., Jilbert, T., Silveira, M., Slomp, C.P., 2014. Redox-dependent changes in manganese speciation in Baltic Sea sediments from the Holocene Thermal Maximum: an EXAFS, XANES and LC-ICP-MS study. Chem. Geol. 370, 49–57. https://doi.org/10.1016/j.chemgeo.2014.01.013.

Lepland, A., Stevens, R.L., 1998. Manganese authigenesis in the Landsort Deep, Baltic Sea. Mar. Geol. 151, 1–25. https://doi.org/10.1016/S0025-3227(98)00046-2.

Li, Y.-L., Vali, H., Yang, J., Phelps, T.J., Zhang, C.L., 2006. Reduction of iron oxides enhanced by a sulfate-reducing bacterium and biogenic H_2S. Geomicrobiol J. 23, 103–117. https://doi.org/10.1080/01490450500533965.

Loyaux-Lawniczak, S., Refait, P., Ehrhardt, J.-J., Lecomte, P., G´enin, J.-M.R., 2000. Trapping of Cr by formation of ferrihydrite during the reduction of chromate ions by Fe(II)– Fe(III) hydroxysalt green rusts. Environ. Sci. Technol. 34, 438–443. https:// doi.org/10.1021/es9903779.

Malinowski, E.R., 1978. Theory of error for target factor analysis with applications to mass spectrometry and nuclear magnetic resonance spectrometry. Anal. Chim. Acta 103, 339–354. https://doi.org/10.1016/S0003-2670(01)83099-3.

Malinowski, E.R., 1987. Theory of the distribution of error eigenvalues resulting from principal component analysis with applications to spectroscopic data. J. Chemom. 1, 33–40. https://doi.org/10.1002/cem.1180010106.

Malinowski, E.R., 1991. Factor Analysis in Chemistry. John Wiley, New York. Manceau, A., Charlet, L., 1992. X-Ray absorption spectroscopic study of the sorption of Cr(lll) at the oxide-water interface. J. Colloid Interface Sci. 148, 425–442. https://

doi.org/10.1016/0021-9797(92)90181-K.Manceau, A., Schlegel, M.L., Musso, M., Sol, V.A., Gauthier, C., Petit, P.E., Trolard, F.,

2000. Crystal chemistry of trace elements in natural and synthetic goethite. Geochim. Cosmochim. Acta 64, 3643–3661. https://doi.org/10.1016/S0016-7037 (00)00427-0.

Marchand, C., Fernandez, J.-M., Moreton, B., Landi, L., Lallier-Verg`es, E., Baltzer, F., 2012. The partitioning of transitional metals (Fe, Mn, Ni, Cr) in mangrove sediments downstream of a ferralitized ultramafic watershed (New Caledonia). Chem. Geol. 300–301, 70–80. https://doi.org/10.1016/j.chemgeo.2012.01.018.

McKenzie, R.M., 1989. In: Dixon, J.B., Weed, S.B. (Eds.), Manganese Oxides and Hydroxides, 2nd ed., Minerals in Soil Environments. Soil Science Society of America, pp. 181–193.

Merkle, R.K.W., Loubser, M., Gra¨ser, P.P.H., 2004. Incongruent dissolution of chromite in lithium tetraborate flux. X-Ray Spectrom. 33, 222–224. https://doi.org/10.1002/ xrs.759.

Merrot, P., Juillot, F., No¨el, V., Lefebvre, P., Brest, J., Menguy, N., Guigner, J.-M., Blondeau, M., Viollier, E., Fernandez, J.-M., Moreton, B., Bargar, J., Morin, G., 2019. Nickel and iron partitioning between clays, Fe-oxides and Fe-sulfides in lagoon sediments from New Caledonia. Sci. Total Environ. 689, 1212–1227. https://doi. org/10.1016/j.scitotenv.2019.06.274.

Morse, J.W., Wang, Q., 1997. Pyrite formation under conditions approximating those in anoxic sediments: II. Influence of precursor iron minerals and organic matter. *Mar. Chem*. 57, 187–193. https://doi.org/10.1016/S0304-4203(97)00050-9.

Motzer, W.E., 2005. Chemistry, geochemistry, and geology of chronium and chromium compounds. In: Guertin, J., Jacobs, J.A., Avakian, C. (Eds.), Chromium (VI) Handbook. CRC Press, Boca Raton, Fla., pp. 23–91

Neretin, L.N., Bo¨ttcher, M.E., Jørgensen, B.B., Volkov, I.I., Lüschen, H., Hilgenfeldt, K., 2004. Pyritization processes and greigite formation in the advancing sulfidization

front in the upper Pleistocene sediments of the Black Sea. Geochim. Cosmochim.

Acta 68, 2081–2093. https://doi.org/10.1016/S0016-7037(03)00450-2.Nico, P.S., Zasoski, R.J., 2000. Importance of Mn(III) availability on the rate of Cr(III)

oxidation on δ-MnO_2. Environ. Sci. Technol. 34, 3363–3367. https://doi.org/

10.1021/es991462j.No¨el, V., Marchand, C., Juillot, F., Ona-Nguema, G., Viollier, E., Marakovic, G., Olivi, L.,

Delbes, L., Gelebart, F., Mori, G., 2014. EXAFS analysis of iron cycling in mangrove sediments downstream a lateritized ultramafic watershed (Vavouto Bay, New Caledonia). Geochim. Cosmochim. Acta 136, 211–228. https://doi.org/10.1016/j. gca.2014.03.019.

No¨el, V., Morin, G., Juillot, F., Marchand, C., Brest, J., Bargar, J.R., Mun˜oz, M., Marakovic, G., Ardo, S., Brown, G.E., 2015. Ni cycling in mangrove sediments from New Caledonia. Geochim. Cosmochim. Acta 169, 82–98. https://doi.org/10.1016/j. gca.2015.07.024.

Noronha-D'Mello, C.A., Nayak, G.N., 2015. Geochemical characterization of mangrove sediments of the Zuari estuarine system, West coast of India. Estuar. Coast. Shelf Sci. 167, 313–325. https://doi.org/10.1016/j.ecss.2015.09.011.

Nriagu, J.O., 1988. A silent epidemic of environmental metal poisoning? Environ. Pollut. 50, 139–161. https://doi.org/10.1016/0269-7491(88)90189-3.

Otero, X.L., Ferreira, T.O., Huerta-Diaz, M.A., Partiti, C.S.M., Souza Jr., V., Vidal- Torrado, P., Macias, F., 2009. Geochemistry of iron and

manganese in soils and sediments of a mangrove system, Island of Pai Matos (Cananeia-SP, Brazil). Geoderma 148, 318–335. https://doi.org/10.1016/j.geoderma.2008.10.016.

Oze, C., Fendorf, S., Bird, D.K., Coleman, R.G., 2004. Chromium geochemistry of serpentine soils. Int. Geol. Rev. 46, 97–126. https://doi.org/10.2747/0020- 6814.46.2.97.

Oze, C., Bird, D.K., Fendorf, S., 2007. Genesis of hexavalent chromium from natural sources in soil and groundwater. PNAS 104, 6544–6549. https://doi.org/10.1073/ pnas.0701085104.

Paquette, J., Reeder, R.J., 1995. Relationship between surface structure, growth mechanism, and trace element incorporation in calcite. Geochim. Cosmochim. Acta 59, 735–749. https://doi.org/10.1016/0016-7037(95)00004-J.

Patterson, R.R., Fendorf, S., Fendorf, M., 1997. Reduction of hexavalent chromium by amorphous iron sulfide. Environ. Sci. Technol. 31, 2039–2044. https://doi.org/ 10.1021/es960836v.

Peterson, M.L., White, A.F., Brown, G.E., Parks, G.A., 1997. Surface passivation of magnetite by reaction with aqueous Cr(VI): XAFS and TEM results. Environ. Sci. Technol. 31, 1573–1576. https://doi.org/10.1021/es960868i.

Prego, R., Caetano, M., Ospina-Alvarez, N., Raimund, J., Vale, C., 2014. Basin-scale contributions of Cr, Ni and Co from Ortegal Complex to the surrounding coastal environment (SW Europe). Sci. Total Environ. 468–469, 495–504. https://doi.org/ 10.1016/j.scitotenv.2013.08.036.

Puzon, G.J., Roberts, A.R., Kramer, D.M., Xun, L., 2005. Formation of soluble organo–chromium(III) complexes after chromate reduction in the presence of cellular organics. Environ. Sci. Technol. 39, 2811–2817. https://doi.org/10.1021/ es048967g.

Puzon, G.J., Tokala, R.K., Zhang, H., Yonge, D., Peyton, B.M., Xun, L., 2008. Mobility and recalcitrance of organo-chromium(III) complexes. Chemosphere 70, 2054–2059. https://doi.org/10.1016/j.chemosphere.2007.09.010.

Qafoku, O., Pearce, C.I., Neumann, A., Kovarik, L., Zhu, M., Ilton, E.S., Bowden, M.E., Resch, C.T., Arey, B.W., Arenholz, E., 2017. Tc (VII) and Cr (VI) interaction with naturally reduced ferruginous smectite from redox transition zone. Environ. Sci. Technol. 51, 9042–9052. https://doi.org/10.1021/acs.est.7b02191.

Quantin, C., Becquer, T., Berthelin, J., 2002. Mn-oxide: a major source of easily mobilisable Co and Ni under reducing conditions in New Caledonia Ferralsols. Compt. Rendus Geosci. 334, 273–278. https://doi.org/10.1016/S1631-0713(02) 01753-4.

R Core Team, 2020. R: A language and environment for statistical computing. R Foundation for Statistical Computing, Vienna, Austria. https://www.R-project.org/. Rai, D., Eary, L.E., Zachara, J.M., 1989. Environmental chemistry of chromium. Sci. Total

Environ. 86, 15–23. https://doi.org/10.1016/0048-9697(89)90189-7.Ravel, B., Newville, M., 2005. *ATHENA*, *ARTEMIS*, *HEPHAESTUS*: data analysis for X-ray absorption spectroscopy using *IFEFFIT*. J. Synchrotron Radiat. 12, 537–541. https://

doi.org/10.1107/S0909049505012719.Richard, F.C., Bourg, A.C.M., 1991. Aqueous geochemistry of chromium: a review. Water

Res. 25, 807–816. https://doi.org/10.1016/0043-1354(91)90160-R. Schmidt, R.L., 1984. Thermodynamic Properties and Environmental Chemistry of

Chromium (No. PNL-4881, 6675931). https://doi.org/10.2172/6675931.Shaw, T.J., Gieskes, J.M., Jahnke, R.A., 1990. Early diagenesis in differing depositional

environments: the response of transition metals in pore water. Geochim. Cosmochim. Acta 54, 1233–1246. https://doi.org/10.1016/0016-7037(90)90149-F.

Slomp, C.P., Malschaert, J.F.P., Lohse, L., Van Raaphorst, W., 1997. Iron and manganese cycling in different sedimentary environments on the North Sea continental margin. Cont. Shelf Res. 17, 1083–1117. https://doi.org/10.1016/S0278-4343(97)00005-8.

Soldati, A.L., Jacob, D.E., Glatzel, P., Swarbrick, J.C., Geck, J., 2016. Element substitution by living organisms: the case of manganese in mollusc shell aragonite. Sci. Rep. 6, 22514. https://doi.org/10.1038/srep22514.

Son, S., Newton, A.G., Jo, K., Lee, J.-Y., Kwon, K.D., 2019. Manganese speciation in Mn- rich CaCO3: a density functional theory study. Geochim. Cosmochim. Acta 248, 231–241. https://doi.org/10.1016/j.gca.2019.01.011.

Stanin, F.T., 2005. The transport and fate of chronium(VI) in the environment. In: Guertin, J., Jacobs, J.A., Avakian, C. (Eds.), Chromium (VI) Handbook. CRC Press, Boca Raton, Fla., pp. 165–214

Stipp, S.L.S., Hansen, M., Kristensen, R., Hochella, M.F., Bennedsen, L., Dideriksen, K., Balic-Zunic, T., L´eonard, D., Mathieu, H.-J., 2002. Behaviour of Fe-oxides relevant to contaminant uptake in the environment. Chem. Geol. 190, 321–337. https://doi. org/10.1016/S0009-2541(02)00123-7.

Stumm, W., Morgan, J.J., 1996. Aquatic Chemistry: Chemical Equilibria and Rates in Natural Waters, third ed. Wiley-Interscience, New York.

Szulczewski, M.D., Helmke, P.A., Bleam, W.F., 2001. XANES spectroscopy studies of Cr (VI) reduction by thiols in organosulfur compounds and humic substances. Environ. Sci. Technol. 35, 1134–1141. https://doi.org/10.1021/es001301b.

Taylor, R.W., Shen, S., Bleam, W.F., Tu, S.I., 2000. Chromate removal by dithionite- reduced clays: evidence from direct X-ray adsorption near edge spectroscopy (XANES) of chromate reduction at clay surfaces. Clay Clay Miner. 48, 648–654. https://doi.org/10.1346/CCMN.2000.0480606.

Tebo, B.M., Bargar, J.R., Clement, B.G., Dick, G.J., Murray, K.J., Parker, D., Verity, R., Webb, S.M., 2004. Biogenic manganese oxides: properties and mechanisms of formation. Annu. Rev. Earth Planet. Sci. 32, 287–328. https://doi.org/10.1146/ annurev.earth.32.101802.120213.

Tebo, B.M., Johnson, H.A., McCarthy, J.K., Templeton, A.S., 2005. Geomicrobiology of manganese(II) oxidation. Trends Microbiol. 13, 421–428. https://doi.org/10.1016/j. tim.2005.07.009.

Thamdrup, B., Fossing, H., Jørgensen, B.B., 1994. Manganese, iron and sulfur cycling in a coastal marine sediment, Aarhus bay, Denmark. Geochim. Cosmochim. Acta 58, 5115–5129. https://doi.org/10.1016/0016-7037(94)90298-4.

Trolard, F., Bourrie, G., Jeanroy, E., Herbillon, A.J., Martin, H., 1995. Trace metals in natural iron oxides from laterites: a study using selective kinetic extraction. Geochim. Cosmochim. Acta 59, 1285–1297. https://doi.org/10.1016/0016-7037 (95)00043-Y.

Ulric, M., Cathelineau, M., Mun˜oz, M., Boiron, M.-C., Teitler, Y., Karpoff, A.M., 2019. The relative distribution of critical (Sc, REE) and transition metals (Ni, Co, Cr, Mn, V) in some Ni-laterite deposits of New Caledonia. J. Geochem. Explor. 197, 93–113. https://doi.org/10.1016/j.gexplo.2018.11.017.

UNESCO, 2008. Lagoons of New Caledonia: reef diversity and associated ecosystems. https://whc.unesco.org/en/list/1115/.

Vincent, B., Jourand, P., Juillot, F., Ducousso, M., Galiana, A., 2018. Biological *in situ* nitrogen fixation by an Acacia species reaches optimal rates on extremely contrasted soils. Eur. J. Soil Biol. 86, 52–62. https://doi.org/10.1016/j.ejsobi.2018.03.003.

Wang, Q., Morse, J.W., 1996. Pyrite formation under conditions approximating those in anoxic sediments I. Pathway and morphology. *Mar. Chem*. 52, 99–121. https://doi. org/10.1016/0304-4203(95)00082-8.

Wang, Y., Van Cappellen, P., 1996. A multicomponent reactive transport model of early diagenesis: application to redox cycling in coastal marine sediments. Geochim. Cosmochim. Acta 60, 2993–3014. https://doi.org/10.1016/0016-7037(96)00140-8.

Webb, S.M., 2005. SIXPack a graphical user interface for XAS analysis using IFEFFIT. Phys. Scr. T115, 1011–1014. https://doi.org/10.1238/Physica.Topical.115a01011. Webb, S.M., Dick, G.J., Bargar, J.R., Tebo, B.M., 2005. Evidence for the presence of Mn

(III) intermediates in the bacterial oxidation of Mn(II). PNAS 102, 5558–5563.

https://doi.org/10.1073/pnas.0409119102.Wedepohl, K.H., 1995. The composition of the continental crust. Geochim. Cosmochim.

Acta 59, 1217–1232. https://doi.org/10.1016/0016-7037(95)00038-2.Williams, A.G.B., Scherer, M.M., 2001. Kinetics of Cr(VI) reduction by carbonate green

rust. Environ. Sci. Technol. 35, 3488–3494. https://doi.org/10.1021/es010579g. World Health Organization (Ed.), 2011. Guidelines for Drinking-water Quality, 4. ed.

World Health Organization, Geneva.Zampella, M., Adamo, P., Caner, L., Petit, S., Righi, D., Terribile, F., 2010. Chromium and

copper in micromorphological features and clay fractions of volcanic soils with andic properties. Geoderma 157, 185–195. https://doi.org/10.1016/j. geoderma.2010.04.012.

Zhitkovich, A., 2011. Chromium in drinking water: sources, metabolism, and cancer risks. Chem. Res. Toxicol. 24, 1617–1629. https://doi.org/10.1021/tx200251t.